



# **POLITECNICO DI TORINO**

*Department of Environment, Land and Infrastructure Engineering*

Master of Science in Petroleum Engineering

## **SENSITIVITY ANALYSIS OF RESERVOIR SIMULATED PRODUCTION CHANGES CAUSED BY WHILE-DRILLING UPDATES**

Supervisor:

Prof. Dario VIBERTI

Co-Supervisors:

Jarle HAUKÅS, Schlumberger Stavanger Research

Diogo SALIM, Schlumberger Stavanger Research

Candidate:

Maria Fernanda RANGEL BARRERA

**JULY 2019**

Thesis submitted in compliance with the requirements for the Master of Science degree

## ABSTRACT

The prediction stage in reservoir simulation is quite important to evaluate production life and thus select future alternatives to improve hydrocarbon recovery. In order to generate appropriate results at this stage, a study of the impact on the dynamic behavior when the static model is updated was developed. The main focus was on a high angle producer well located in one of the compartments of the full-field reservoir model, with the purpose of analyzing water breakthrough coming from the injection well and how subsurface data acquired while-drilling can help reduce model uncertainty.

This thesis is focused on the modification of static petrophysical properties, namely porosity and permeability, using tools provided by the Petrel E&P software. Initially, well log data from some of the wells in the compartment was analyzed. Subsequently, a refinement of the grid along the selected production well was introduced, followed by a property update within the refined grid based on the log data acquired.

A forecast was carried out mainly focusing on a newly drilled producer (high angle well) within the compartment for a selected simulation period of eight years. This prediction was based on field development strategy in which some individual constraints were set up for each well. At the same time, some group controls were defined in relation to reservoir volume production and injection rates.

Sensitivity analysis was performed using INTERSECT, for each of the property updates individually and for all property updates combined. Furthermore, the impact of varying the properties with a smaller region just around the wellbore was considered. A final analysis was carried out by closing one of the perforations of the producer well to evaluate the potential for improving production given the estimated water breakthrough characteristics within the simulated period.

Results showed that decreasing the porosity and increasing the permeability around the producer well, slightly anticipates the effect of water breakthrough. When the two properties were added simultaneously, the water influx comes a year and a half earlier with respect to the Base case, which is expected considering the overall impact.

Moreover, it was concluded that the water front moves from the injection well towards the north of the producer, reaching all the perforations more or less on the same date. Consequently,

advanced technologies for controlling water influx, like inflow control devices (ICD), located at different segments of the producer well would be appropriate.

## ACKNOWLEDGEMENTS

Firstly, I express my gratitude to God.

I would like to thank my supervisor, Professor Dario Viberti, for the support and collaboration during this process, always being able to help and ensuring a successful completion of the work.

Special thanks to the Schlumberger Stavanger Research family, principally to Massimo Virgilio and my co-supervisors, Jarle Haukås and Diogo Salim. Whom always were ready to collaborate, showing passion and dedication in their work, without them this achievement will not be possible. Thank you very much for all the explanations and time devoted to the students. In addition, to Jan Øystein Haavig Bakke for his contribution to this project and, Gabriela Nass, Marie Etchebes and Aicha Bounaim, for their support and collaboration during the process. This experience really taught me how successful you can be when you have an excellent teamwork.

I would also like to greatly thank to Equinor for providing all the data require to develop this thesis.

To my beloved family, all my triumphs are for them. Likewise, to Felipe and my close friends, many thanks for their support and encouragement.

Finally, to the master's squad, it was a really great time shared in Stavanger.

**NOMENCLATURE**

<u>Symbol</u>	<u>Definition</u>
$\Phi$	Porosity
$C$	Compressibility
$P$	Pressure
$K$	Permeability
$v$	Fluid velocity
$d_p/d_l$	Pressure gradient in the direction of the flow
$\lambda$	Relative mobility of fluid
$\partial/\partial_x$	Derivative in $x$ direction
$\rho$	Density
$B$	Volumetric Factor
$R_s$	Solution gas-oil ratio
$S$	Saturation
$a$	Tortuosity factor
$R$	Resistivity
$c$	Cementation exponent
$n$	Saturation exponent
$dS$	Difference in saturation
$mD$	Millidarcy
$m$	Meters
$cP$	Centipoise
$P_b$	Bubble pressure
$t$	Time
$\Delta P$	Delta of pressure
$r$	Relative
$V$	Volume

## Subscripts

<u>Symbol</u>	<u>Definition</u>
<i>h</i>	Horizontal
$x = i$	Horizontal direction
$y = j$	Horizontal direction
<i>k</i>	Vertical direction
<i>T</i>	Total
0	Initial
<i>w</i>	Water
<i>o</i>	Oil
<i>g</i>	Gas
<i>sc</i>	Standard conditions
<i>fl</i>	Fluid
<i>ma</i>	Matrix
<i>B</i>	Bulk
<i>sh</i>	Shale
<i>Re</i>	Reservoir
<i>wf</i>	Wellbore (bottom hole) flowing pressure

## Abbreviations

<u>Symbol</u>	<u>Definition</u>
<i>BHP</i>	Bottom hole pressure
<i>LGR</i>	Local grid refinement
<i>LWD</i>	Logging while-drilling
<i>MRGC</i>	Multi-dimensional dot-pattern recognition method
<i>PVT</i>	Pressure, volume, temperature
<i>THP</i>	Tubing head pressure
<i>WBT</i>	Water breakthrough
<i>GOR</i>	Gas-oil ratio

**CONTENTS**

ABSTRACT ..... ii

ACKNOWLEDGEMENTS ..... iv

NOMENCLATURE ..... v

    Subscripts..... vi

    Abbreviations..... vi

LIST OF FIGURES ..... x

LIST OF TABLES .....xiii

1. INTRODUCTION ..... 1

    1.1. Scope of Work ..... 2

2. RESERVOIR SIMULATION BACKGROUND ..... 3

    2.1. Geological Model Development ..... 3

        2.1.1. Data Collection..... 4

        2.1.2. Gridding Selection ..... 5

    2.2. Reservoir Rock and Fluid Properties ..... 6

        2.2.1. Rock Properties ..... 6

        2.2.2. Fluid Properties ..... 8

    2.3. Modeling Flow in the Porous Media ..... 8

        2.3.1. Radius of investigation..... 10

3. HISTORY MATCHING AND FORECASTING ..... 11

    3.1. Reservoir performance prediction..... 11

        3.1.1. Boundary conditions ..... 11

        3.1.2. Constraints and actions ..... 12

        3.1.3. Validity of model predictions..... 12

4. SOFTWARE..... 14

    4.1. Petrel E&P ..... 14

    4.2. INTERSECT ..... 14

5. LOGGING WHILE DRILLING (LWD) .....	15
5.1. Overcoming limitations in Horizontal Drilling.....	15
5.2. Petrophysics fundamentals.....	16
5.2.1. Porosity Estimation .....	16
5.2.2. Water Saturation.....	17
5.2.3. Permeability Estimation .....	17
6. CASE STUDY.....	18
6.1. High Angle Well (Producer well) .....	20
7. METHODOLOGY .....	22
7.1. Updating of the well completions .....	22
7.2. Local grid refinement around the well.....	23
7.3. Updating of the properties .....	23
7.3.1. Well log upscaling and petrophysical modeling .....	24
7.4. Creation of the field management strategy prediction.....	26
7.5. Set up of the prediction cases.....	27
8. RESULTS.....	29
8.1. Sector model with gridding refinement (Base case).....	29
8.1.1. Field performance .....	29
8.1.1. Bottom hole pressure and production rates in the producer.....	31
8.1.2. Influence of the saturation of gas on the producer well prediction since start-up of production.....	31
8.1.3. Water Saturation changes.....	32
8.2. Sector model with LGR and porosity updates (Case 1).....	32
8.2.1. Pore volume changes.....	33
8.2.2. Field performance .....	33
8.2.3. Bottom hole pressure and production rates in the producer.....	34
8.2.4. Difference in water saturation ( $dS_w$ ) at the beginning of the prediction .....	35

8.3.	Sector model with LGR and permeability updates (Case 2).....	36
8.3.1.	Permeability variations in the LGR.....	36
8.3.2.	Field performance .....	37
8.3.3.	Bottom hole pressure and production rates in the producer.....	38
8.3.4.	Water front behavior .....	39
8.4.	Sector model with LGR and porosity and permeability updates (Case 3).....	39
8.4.1.	Field performance .....	39
8.4.2.	Bottom hole pressure and production rates in the producer.....	41
8.4.3.	Water saturation changes .....	41
8.4.4.	Water flow rates in each perforation .....	42
8.5.	Updates only within polygon close to the well (Case 4) .....	44
8.5.1.	Pore volume variations.....	45
8.5.2.	Permeability variations.....	45
8.5.3.	Field performance .....	46
8.5.4.	Bottom hole pressure and production rates in the producer.....	47
8.5.5.	Water front behavior .....	47
8.5.6.	Water flow rates in each perforation .....	48
8.6.	Impacts on the WBT for different perforation scenarios .....	51
9.	DISCUSSION.....	52
10.	CONCLUSION AND FURTHER STUDIES .....	56
10.1.	DepoGrid Construction .....	57
11.	REFERENCES .....	59
	Appendix I .....	62
	Appendix II.....	64
	Appendix III.....	66

**LIST OF FIGURES**

Figure 2-1 Stratigraphic grids, (Lie & Mallison, 2013). ..... 5

Figure 5-1 The uncalibrated model, created prior to drilling, is calibrated with the properties classified from the LWD logs as new measurement, example in geosteering applications, (Pedersen, Tennebo, Sonneland, & Carrillat, 2005). ..... 16

Figure 6-1 Histogram of porosity distribution in the reservoir model (Values in %). ..... 18

Figure 6-2 Histogram of horizontal permeability distribution in the reservoir model (Units in mD). ..... 19

Figure 6-3 Sector model injection history. .... 20

Figure 6-4 Location of the high angle well in the Upper Brent. .... 21

Figure 6-5 Fault crossing through the producer well. .... 21

Figure 7-1 Completion design of the high angle well (producer well). .... 22

Figure 7-2 Local grid refinement around the producer well. .... 23

Figure 7-3 Producer well logs (Porosity, permeability, water saturation and volume of shale). ..... 24

Figure 7-4 Porosity updates in the local grid (left: No updates, right: Porosity updates). .. 25

Figure 7-5 Permeability updates in i and j direction in the local grid (left: No updates, right: Permeability updates). .... 26

Figure 7-6 VFP (Hydraulic table) used in the prediction strategy for the producer well... 27

Figure 7-7 Porosity and permeability (i and j direction) updates inside the polygon. .... 28

Figure 8-1 Dynamic pressure behavior in the sector model with local grid refinement in j direction (years 1999, 2017 and 2025) ..... 29

Figure 8-2 Dynamic pressure behavior in the sector model with LGR in k direction, layer number 5 (years 1999, 2017 and 2025). .... 29

Figure 8-3 Field pressure and, cumulative injection and production for the Base case. .... 30

Figure 8-4 Production rates in the high angle well (historical and prediction case). .... 31

Figure 8-5 Saturation of gas in the historical case (k direction)..... 31

Figure 8-6 Water saturation changes in j direction in the Base case model (years 1999, 2017 and 2025) ..... 32

Figure 8-7 Water saturation changes in the Base case model for the years 1999, 2017 and 2025 (layer 8, k direction)..... 32

Figure 8-8 Pore volume before and after the update of the property (layer number 5). .... 33

Figure 8-9 Dynamic pressure behavior in the sector model at the years 1999, 2017 and 2025. .... 33

Figure 8-10 Field pressure and, cumulative injection and production for the Base case and Case 1..... 34

Figure 8-11 Bottom hole pressure and production rates in the high angle well considering porosity updates. .... 34

Figure 8-12 dSw before and after property modifications (Base case and Case 1 respectively at the end of the historical case, beginning of the forecasting)..... 35

Figure 8-13 Comparison of Sw in the Base case (left) and Case1 (right) in 2025..... 36

Figure 8-14 Permeability i direction (layer number 5 of the LGR). .... 36

Figure 8-15 Dynamic pressure changes at the starting of the production, beginning and ending of the forecasting (1999, 2017 and 2025 respectively)..... 37

Figure 8-16 Field pressure and, cumulative injection and production for the Base case and Case 2..... 37

Figure 8-17 Bottom hole pressure and production rates in the high angle well with permeability updates. .... 38

Figure 8-18 Water displacement in the prediction case for the years 1999, 2017 and 2025 (j direction)..... 39

Figure 8-19 Water front behavior in the Case 2 for the years 1999, 2017 and 2025 (layer 8, k direction)..... 39

Figure 8-20 Distribution of dynamic pressure at the beginning of the production and during the prediction time (1999, 2015 and 2017 correspondingly)..... 39

Figure 8-21 Field pressure and, cumulative injection and production for the Base case and Case 3..... 40

Figure 8-22 Bottom hole pressure and production rates in the high angle well, Base case and with property updates (Case 3). .... 41

Figure 8-23 Water saturation changes in the Case 3 for the years 1999, 2017 and 2025 (layer 8, k direction)..... 41

Figure 8-24 Water flow rate from the segments associated with perforation number 1. .... 42

Figure 8-25 Water flow rate from the segments associated with perforation number 2. .... 43

Figure 8-26 Water flow rate from the segments associated with perforation number 3. .... 43

Figure 8-27 Water flow rate from the segments associated with perforation number 4. .... 44

Figure 8-28 8 Pore volumes before and after the update of the property (layer number 5).45

Figure 8-29 Permeability values in i direction (Layer 5, k direction). .... 45

Figure 8-30 Dynamic pressure changes in the years 1999, 2017 and 2025 respectively... 46

Figure 8-31 Field pressure and, cumulative injection and production for the Base case and Case 4..... 46

Figure 8-32 Bottom hole pressure and production rates comparison between the Base Case, Case 3 and Case 4. .... 47

Figure 8-33 Water front behavior in the Case 4 for the years 1999, 2017 and 2025 (layer 8, k direction). .... 47

Figure 8-34 Water flow rate for each segment located in the perforation number 1. .... 48

Figure 8-35 Water flow rate for each segment located in the perforation number 2. .... 49

Figure 8-36 Water flow rate for each segment located in the perforation number 3. .... 49

Figure 8-37 Water flow rate for each segment located in the perforation number 4. .... 50

Figure 8-38 Water breakthrough comparison when perforation 4 is closed since the beginning of the production..... 51

Figure 10-1 Construction of the DepoGrid for the sector model (Marie Etchebes, 2018).. 58

Figure 11-1 Completion of the high angle well (producer well)..... 62

Figure 11-2 Well segmentation setup for the simulation runs. .... 63

**LIST OF TABLES**

Table 2-1 Data desired in order to fulfill the requirements to populate correctly the model, (Gilman & Ozgen, 2013). ..... 3

Table 7-1 Rates and pressure controls in the producer well..... 27

Table 7-2 Rate and pressure control in the injection well. .... 27

Table 8-1 Pore volume changes in layer number 5 (k direction) ..... 33

## 1. INTRODUCTION

Reservoir simulation has been used over the years to describe and optimize the future production of a field, based on a careful construction and followed calibration of the model involving the use of multiple data. Geological information and data have an important role in determining the areas where hydrocarbons may be present. PVT (Pressure, Volume, and Temperature) and petrophysical properties are used to populate the model in a more accurate way and finally, with drilling and completion information from the wells allocated in the reservoir, it is possible to develop more realistic predictions.

In the last decades, horizontal and high angle wells have been drilled to maximize hydrocarbon production, especially in offshore projects in which the investment is considerably higher. These projects require the development and application of new and advanced technologies in order to optimize the recovery process, reduce structural uncertainties and also allow the updating of the geological model for further studies (Shtun et al., 2017). To obtain a representation as similar as possible to that of the real subsurface setting, a wide range of measurements can be used to constrain a reservoir simulation model. The updates derived from seismic acquisition and interpretation, which considers the dynamic variations in the reservoir and while-drilling measurements, including well logs, can result in significant changes to the pre-drill structural model, such as thickness and extent of the drainage or injection area. Moreover, the original formation evaluation of the reservoir can be modified with more precise rock properties, including the redistribution of the petrophysical and fluid properties from data acquired while-drilling. Such variations in both, the structure and properties, will influence the production estimates obtained from the reservoir simulation model.

Following the model construction and updating of static properties, the history matching is performed with the assistance of advanced computational tools, 4D seismic and well data. Generating results that should correspond with the behavior of the reservoir to facilitate production analysis.

Once the history match is satisfactory performed, the last step is the creation of a prediction case. This case has to meet the needs and characteristics of the specific model. Creating a picture of the production behavior during a certain period of time to evaluate what would be the best possible scenario considering all the constraints. It must be emphasized that there is not a unique solution to generate a forecasting and considerable uncertainty will always exist. Nevertheless, it is the most effective option for decision-making in the oil and gas sector.

## **1.1. Scope of Work**

The main objective of this project is to investigate how data acquired while drilling in a high angle well can be used to update a reservoir model and reduce uncertainty, mainly focusing on the updates and refinement of the porosity and permeability properties in the simulation grid. Furthermore, an objective was to study, through some sensibility analysis, the impact on the estimated reservoir production using diverse software tools as the Petrel E&P Platform, which is focused on the static model building and INTERSECT, that is used for dynamic simulation, especially in the case of the presence of local grid refinements.

The first chapters are devoted to the theoretical background of reservoir simulation and logging-while-drilling. Chapter number 6 illustrates the case study, while chapter 7 explains in detail how the static model was updated using drilling reports, completion information and data from logs, provided by the client. Chapter 8 shows developed simulation runs with respective results. The study is finalized with chapters 9 and 10, which are dedicated to the discussion, improvements, and further studies.

## 2. RESERVOIR SIMULATION BACKGROUND

Oil and gas companies are looking for more accurate predictions of the reservoir model to optimize production and obtain as much information as they can to be able to recognize any potential sector of reservoirs rich in hydrocarbons. Reservoir simulation is an advanced tool that allows the study of not just an initial volume of oil in place, but also the dynamic behavior that governs the fluid using mathematical equations. For this, it is necessary to have good quality data, including historical production, geological and geophysical information, to develop an accurate history matching and forecasting.

It is virtually impossible to obtain the exact dynamic response to what is happening in the reservoir, because of measurement and model uncertainty. That is why it is very important to consider the reliability of the information obtained from the running of real time tools to elaborate a correct visualization of the scenery existing at the subsurface level.

### 2.1. Geological Model Development

The objective of the reservoir characterization is to determine the spatial distribution of the petrophysical properties conditioned to the available static data (Da Veiga & Ravalec-Dupin, 2010). It is extremely important to create a static model to be run in a numerical simulator that describes the most rigorous interpretation of the reservoir. The construction of this model is developed with data collected (Table 2-1) that allows a 3D characterization of the entire reservoir performing not just a good history match but also honoring all available data to enable correct future analysis.

*Table 2-1 Data desired in order to fulfill the requirements to populate correctly the model, (Gilman & Ozgen, 2013).*

<u>Geological interpretation</u>	By means of outcrop, cross sections, analogy, and expert opinion to understand the depositional environment and architectural elements.
<u>Well logs</u>	Stratigraphic top picks must be consistent with geologic and seismic interpretations, and log traces must be normalized and processed in a consistent manner over the entire area of interest.
<u>Cores</u>	Are required to understand geologic controls such as facies descriptions and provide basic flow

	characterization such as porosity, permeability, and relative permeability.
<u>Geochemistry and PVT analysis</u>	May provide data for compartmentalization and compositional grading estimates. PVT data are also required for fluid characterization.
<u>Seismic data</u>	Can be integrated with various interpretations for structural analysis and possibly for property distribution using various seismic attributes. These interpretations must be consistent with geologic and petrophysical interpretations.
<u>Drilling records and well completions</u>	Must be carefully checked. Perforations should be in the correct intervals when loaded into the 3D model.
<u>Production/injection profiles</u>	Can provide information about heterogeneity and compartmentalization before any dynamic simulation is performed.
<u>Production history and pressure data</u>	Can also be compared with geologic/geophysical interpretations to provide much insight before dynamic simulation.

### 2.1.1. Data Collection

To create a geological model that fulfill all the requirements, there are different sources from which the data can be gathered. Seismic surveys are one of the most common sources used to identify the faults and how extended is the reservoir, as well as the identification of present fractures and determination of the horizons for the static model. The main drawbacks are the time-consuming process of the seismic interpretation and the high costs associated with the acquisition, adding that the resolution is limited (Lie, 2014). On the other hand, there are the logs, obtained from the run of some tools into the well to acquire data from the vicinities of the wellbore. This data acquired can be quite accurate, but it is given just for a limited radius around the well. Using all the information collected from different sources, like the ones previously mentioned, the engineers can create a reservoir model as similar as possible to the original one.

### 2.1.2. Gridding Selection

There are multiple options when choosing which one is the best grid to develop future reservoir simulations. The most important items to consider for the design of the simulation grid are first, the vertical layering, related with the depositional environment and stratigraphy, second, the grid orientation, contemplating parameters as permeability as a vector property, and third, the grid size, which describes how accurately pressure and saturation fronts can be represented.

In the oil and gas industry the preferred option is stratigraphic grid, that is recognized because it describes the reservoir taking into account the sediments beds conformed by a mixture of multiple particles. The thickness and inclination of each lateral bed can differ due to deposition and compaction process through time, which are geological processes that can trigger the development of fractures and faults. For reservoir simulation purposes fractures are known as cracks existing in the rock, but without generating any displacing of the layers. On the other hand, the faults are fractures that can generate a displacement. The most popular type of grid is called the corner point grid, which consists of hexahedral cells that can be numbered using (i, j, k) notation, (Lie & Mallison, 2013). Figure 2-1 illustrates how a corner-point reservoir model can be visualized in 3D and as a cross-section.

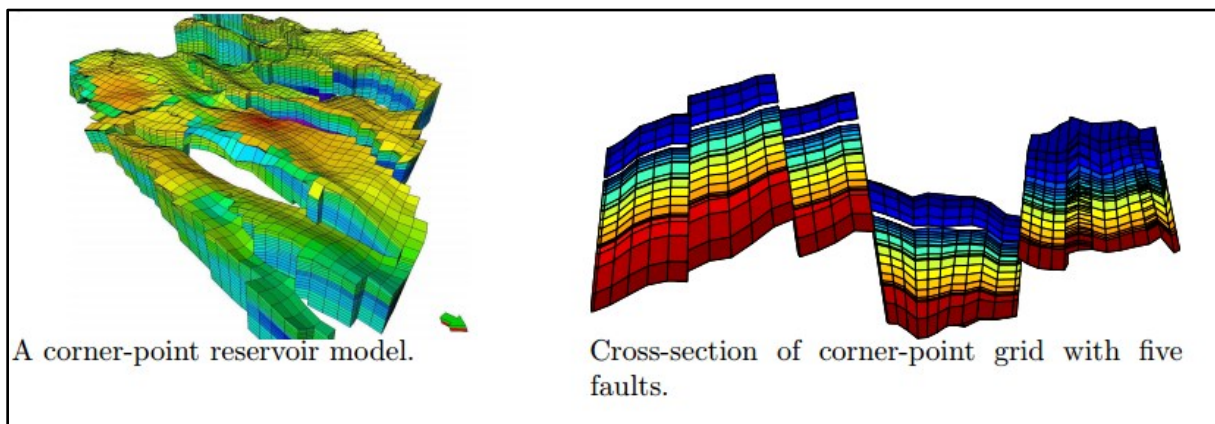


Figure 2-1 Stratigraphic grids (Lie & Mallison, 2013).

### Local Grid Refinement (LGR)

Local refinements enhance the grid definition in areas of a model that requires a higher level of simulation accuracy. To focus on some regions of major interest in complex reservoirs and avoid having to make a refinement in the entire reservoir model that can introduce some unwanted limitations, like computational costs, the local grid refinement can be a good option for future analysis. A local grid refinement can be used to have high resolution in both areal

and vertical direction of the flow behavior. Examples in which LGR has an important role are, the area around a producing well or oil reservoirs connected by a common aquifer (Wasserman, 1987). In chapter 7, it is shown to see how an LGR is applied around the high angle well in order to have a higher accuracy in the main areas of the present study.

## 2.2. Reservoir Rock and Fluid Properties

Rock and fluid properties have a strong influence on the multiphase flow in porous media, as well as the interaction between them, especially for reservoir simulation scenarios. The following sections explain the general concept of the properties that in the subsequent chapters will be described in a more detail way.

### 2.2.1. Rock Properties

A hydrocarbon reservoir is characterized by pores in which the fluids are trapped. In the model it is important to understand how the rock properties affect the fluids flow. This section covers the most important rock properties to be considered in the model updating.

#### Porosity

The pore space in the reservoir rock contains fluids. Some of these pores are characterized by being isolated, while others are interconnected. The ratio between the pore spaces in a rock to the total volume of the rock sample is called porosity. Two primary types of porosity can be found: Total porosity, characterized by considering the isolated and interconnected pores, and the effective porosity, which takes into consideration the interconnected pores. For reservoir simulation purposes, the effective porosity is the one implemented, because only interconnected pores are the ones that produce fluids. Therefore, it is possible to say that the effective porosity is a measure of the reservoir rock's ability to store producible fluids (Ertekin, Abou-Kassen, & King, 2001).

Porosity is dependent on pressure due to the rock compressibility, and it can be defined as:

$$\Phi = \Phi^0 [1 + C_\Phi (P - P^0)], \quad (2.1)$$

where  $P^0$  is the reference pressure at which the porosity is equal to  $\Phi^0$ . This reference pressure is defined as the initial reservoir pressure or the atmospheric one. The equation 2.1 shows that porosity decrease in relation to the reference porosity happens when the pore pressure also decreases, this occurs in primary production, where pressure declines.

## Permeability

Permeability describes the capacity of transmitting fluids through a porous media. When the medium is completely saturated for a single phase is possible to talk about absolute permeability. On the other hand, when the porous medium is saturated with more than one phase, the relative permeability is introduced to describe the reservoir capacity to transmit this specific phase with respect to the others in the porous media.

This property changes from one to another point, depending also on the flow direction. For practical uses, the permeability can be represented in the three principal directions (x, y, and z). In most of the cases the  $K_h = K_x = K_y$  in the horizontal planes, while the vertical permeability,  $K_v$ , is often different from the ones previously mentioned, since even a small presence of a thin layer of shale can change significantly the effect of this permeability. A reservoir in which the permeability is different in different directions is called anisotropic.

The fluid flow equation most used in the gas and oil field to measure the permeability of a core was developed by Henry Darcy and can be expressed as a differential form (Tiab & Donaldson, 2015):

$$v = -\frac{K d_p}{\mu d_l}, \quad (2.2)$$

where  $v$ = fluid velocity( $cm/s$ ),  $K$ = permeability of the porous rock (*Darcy*),  $\mu$ = viscosity (*centipoise*) and  $d_p/d_l$ = pressure gradient in the direction of the flow( $atm/cm$ ).

Another important definition derived from this rock property is the transmissibility. This parameter is defined as the water, oil and gas masses flow in a porous media. Depends on grid discretization and permeability. Transmissibility will be an important factor during the permeability modifications in the current thesis (Cordazzo, Maliska, & Silva, 2002).

## Upscaling of properties

In the static model, one of the challenges is the description of the heterogeneous medium from one scale to another. A specific property is observed at one scale on a specific volume of measurement, but also this value is needed on a different volume size at a different location. The upscaling in reservoir simulation is principally referred to scale up from a geological grid to a reservoir grid. For this type of process geostatistical methods are capable of calculate more values than can simply be distributed and upscale in the model for the simulation. The most used methods are: power-law averaging methods, arithmetic, geometric and harmonic

techniques. This process allows to scale properties from a fine grid to a coarse grid. Currently, for more detail study proposes also downscaling takes place in order to analyze the impact of the refinement in the properties (Islam, Mousavizadegan, Mustafiz, & Abou-Kassem, 2010).

One of the most used algorithms and applied in this study is kriging. This method is highly characterized for an optimal handle of irregular data, providing the means to compute estimation variance which can be used to avoid suboptimal convergence and the extension to represent multi-dimensional data (Landa & Güyagüler, 2003).

### **2.2.2. Fluid Properties**

The most essential fluid properties in reservoir modeling are the fluid compressibility and gas compressibility factors, the solution gas/liquid ratios, fluid formation volume factors and fluid viscosities.

The oil, gas, and water coexist in the reservoir at pressure and temperature equilibrium and can be produced simultaneously from the hydrocarbon reservoirs. The produced gas is the sum of dissolved gas and free gas. The solution gas, comes mostly from the dissolved in oil and the remainder from gas dissolved in water. Consequently, contemplating that oil and water are immiscible fluids, the major effect in the properties of the oil is based on the gas dissolved. For black-oil systems, neither oil nor water vaporize in gas are present in an important amount. For such systems, the presence of oil and water, do not have any effect on the properties of the gas at reservoir conditions (Ertekin et al., 2001).

### **2.3. Modeling Flow in the Porous Media**

In reservoir modeling, mathematical formulation of the flow equations takes into consideration all fluid components that are present there, initial and boundary conditions and other relations to have a detail description of the behavior of the flow. These flow equations are based on the mass-conservation, Darcy's law, and state equations. Further relationships are included, like phase-saturations and capillary pressures as a function of phase-saturation, and these play an important role in the flow modeling.

For reservoir simulation proposes, this thesis will be focused on the black-oil modeling of hydrocarbon reservoirs, mainly in a three-phase flow of oil, water, and gas. Black oil simulations solve multiphase, multidimensional flow equations for fluids in which the properties are dependent on pressure. The flow equations for the three phases are given taking into consideration the fluxes and concentrations of the conservation equations for each component in each of the three phases (Fanchi, 2005).

The following equations represent the basic fluid flow equations for a black oil simulator. Starting from the velocity, assumed as Darcy velocity, the equation in the x component is:

$$v_{xo} = -K_X \lambda_o \frac{\partial}{\partial x} \left[ P_o - \frac{\rho_w g z}{g_c} \right] \quad (2.3)$$

$$v_{xw} = -K_X \lambda_w \frac{\partial}{\partial x} \left[ P_w - \frac{\rho_w g z}{g_c} \right] \quad (2.4)$$

$$v_{xg} = -K_X \lambda_g \frac{\partial}{\partial x} \left[ P_g - \frac{\rho_o g z}{g_c} \right] \quad (2.5)$$

where  $g$  is the acceleration of gravity in  $m/s^2$ ,  $g_c$  is  $9.8 m/s^2$ ,  $\rho$  denotes density and  $\lambda$  the relative mobility of the fluid.

Phase density is related to formation volume factor and gas solubility by:

$$\rho_o = \frac{1}{B_o} [\rho_{osc} + R_{so} \rho_{gsc}] \quad (2.6)$$

$$\rho_w = \frac{1}{B_w} [\rho_{wsc} + R_{sw} \rho_{gsc}] \quad (2.7)$$

$$\rho_g = \frac{\rho_{gsc}}{B_g} \quad (2.8)$$

And, the saturations satisfy the next constraint:

$$S_o + S_w + S_g = 1 \quad (2.9)$$

Combining certain equations is possible to obtain a mass conservation equation for each component:

$$-\left[ \frac{\partial}{\partial x} \left( \frac{v_{xo}}{B_o} \right) + \frac{\partial}{\partial y} \left( \frac{v_{yo}}{B_o} \right) + \frac{\partial}{\partial z} \left( \frac{v_{zo}}{B_o} \right) \right] - \frac{q_o}{\rho_{osc}} = \frac{\partial}{\partial t} \left( \Phi \frac{S_o}{B_o} \right) \quad (2.10)$$

$$-\left[ \frac{\partial}{\partial x} \left( \frac{v_{xw}}{B_w} \right) + \frac{\partial}{\partial y} \left( \frac{v_{yw}}{B_w} \right) + \frac{\partial}{\partial z} \left( \frac{v_{zw}}{B_w} \right) \right] - \frac{q_w}{\rho_{wsc}} = \frac{\partial}{\partial t} \left( \Phi \frac{S_w}{B_w} \right) \quad (2.11)$$

$$\begin{aligned}
& -\frac{\partial}{\partial x} \left( \frac{v_{xg}}{B_g} + \frac{R_{so}}{B_o} v_{xo} + \frac{R_{sw}}{B_w} v_{xw} \right) - \frac{\partial}{\partial y} \left( \frac{v_{yg}}{B_g} + \frac{R_{so}}{B_o} v_{yo} + \frac{R_{sw}}{B_w} v_{yw} \right) \\
& - \frac{\partial}{\partial z} \left( \frac{v_{zg}}{B_g} + \frac{R_{so}}{B_o} v_{zo} + \frac{R_{sw}}{B_w} v_{zw} \right) - \frac{q_g}{\rho_{gsc}} = \frac{\partial}{\partial t} \left[ \Phi \left( \frac{S_g}{B_g} + R_{so} \frac{S_o}{B_o} + R_{sw} \frac{S_w}{B_w} \right) \right]
\end{aligned} \tag{2.12}$$

for oil, water and gas respectively.

### 2.3.1. Radius of investigation

An important concept introduced in transient well testing analysis to know how far the wave propagation has traveled in the reservoir is the radius of investigation, a relation between time and distance for a given mobility. The most common definition is connected to the circular area where flow would reach pseudo-steady state at a specified time (Kamal & Abbaszadeh, 2009):

$$r_d = 0.029 \sqrt{\frac{Kt}{\Phi \mu C_T}} \tag{2.13}$$

where  $K$  is the permeability,  $t$  time that the wave propagation has traveled,  $\Phi$  porosity,  $\mu$  viscosity, and  $C_T$  total compressibility.

Equation 2.13 assumes a radial homogeneous flow and does not consider the gauge resolution, the overall quality and noise level of the pressure response. Consequently, this definition has to be carefully used in the presence of complex configurations as fractured wells, horizontal wells, and heterogeneous formations, among others.

### **3. HISTORY MATCHING AND FORECASTING**

Reservoir simulation studies consist of two important aspects: Matching historical performance to calibrate the flow model and making predictions (Mattax & Dalton, 1990). History match is the process in which the flow model is calibrated by verifying and refining the reservoir parameters. In order to adjust this, some modifications in the initial reservoir description are done by making reasonable changes in input data until a realistic match is obtained. This phase of the study integrates reservoir geoscience and engineering data branches (Fanchi, 2002). Following this, the prediction takes place to prepare a forecast base on the present operating field strategy and the future evaluation of multiple scenarios. This thesis is mainly focused on the prediction part of the analysis.

#### **3.1. Reservoir performance prediction**

The first step after the calibration has been completed is to prepare a base case prediction. This case is mostly a forecast that will be compared to another hypothetical forecast to determine the most suitable one for the specific reservoir study. The base case is most of the times a continuity of the existing operation conditions, but this can change if there is a better reservoir management scenario that can suit the study. Comparing against the base case scenario, multiple operating strategies can be tested, and a sensitivity analysis can be performed to provide a better understanding of the uncertainty associated with predictions (Fanchi, 2005).

Predictions are valuable for several purposes. The first one is associated with a better interpretation of the reservoir behavior and model sensitivity to changes in the input data. Furthermore, predictions allow companies to estimate the productive life of the reservoir, recovery versus time, considering not just the flow behavior of the reservoir, but also the economic and commercial constraints (Gilman & Ozgen, 2013). Overall, the main idea of developing a forecasting is the possibility to create future reservoir management plans depending on the characteristics of the reservoir. The following sections explain the most important criteria to take into consideration when a prediction case is going to be developed.

##### **3.1.1. Boundary conditions**

Production wells can be constrained by a minimum flowing BHP (Bottom hole pressure) value or equally. If the wells are flowing under natural flow conditions, hydraulic flow tables are needed for the forecasting. Vertical flow behavior can be represented using the existing wells and the available flow-test data related to reservoir fluids, well deviations, tubing parameters, among others. Any of the tables generated has to cover all the THP (Tubing head

pressure) values, water cut, gas-oil ratio and liquid rates projected in the forecast. When the tubing parameters for more than one well are the same, it is possible to group these wells in order to diminish the number of hydraulic tables in the simulation case (Gilman & Ozgen, 2013).

### **3.1.2. Constraints and actions**

In the field, dynamic constraints for injection and production wells are used to limit the maximum flow rate. Related with the producer wells, limits on oil, gas and water production are the most important ones, related to the facilities and pipelines restrictions. For injection wells, parameters like injection rate limits as a function of the pressure, are the most commonly applied constraints when a field strategy is being created. Moreover, injection constraints can limit the phase production rates.

In addition to these controls that are set as an upper limit that cannot be violated a target can be specified at field levels. An example is the oil, gas, or water production target that follows the objective of the production operation. To honor the specified objective rate of the produced phase selected, the simulator first calculates the production potential of the wells based on the BHP or THP limit to select the best strategy to satisfy the controls set for the wells (Gilman & Ozgen, 2013).

### **3.1.3. Validity of model predictions**

Salari (Salari, 1993) studied the veracity of the predictions making a comparison between the actual field performance with the prediction one. The global match in the performance of the total rate and pressure behavior is realistic. However, the field match is somewhat ambiguous, due to the fact that the veracity of the individual performance forecast of the wells differs widely, which allows to arrive to the following conclusions:

- “Barring major geologic and/or reservoir data limitations, fieldwide cumulative production forecast accuracies would tend to range from 10% to 40%.” (Salari, 1993).
- “Well performance forecasts are bound to be less successful than fieldwide predictions.” (Salari, 1993).

These arguments highlight that the history match procedure does not bring a unique solution and therefore, forecast of the reservoir behavior depends of the accuracy of this match.

Although, there is a significant uncertainty associated with reservoir simulation forecasting, this method still being the most reliable in comparison with others, such as decline curves and material balance analysis, to perform and study the reservoir performance. This is especially the cases that do not have much historical information or for cases in which a change in the management strategy is going to be developed (Fanchi, 2005).

## **4. SOFTWARE**

Selection of the software to create the static reservoir model and simulate the dynamic flow path is a key point to focus on order to obtain realistic results. The software described below takes into consideration important points, like the construction of complex static models with multiple presences of faults and compartments. In the case of the numerical simulator, robustness, efficiency, facility of use and modeling of sector refinement areas with geological, properties and resolution improvements, are crucial characteristics of the simulator that improves the accuracy of future predictions.

### **4.1. Petrel E&P**

Petrel E&P platform allows a multidisciplinary workflow to integrate a multitude of data to build complex reservoirs, from prestack processing to advance reservoir modeling, in order to facilitate history matching and further analysis. The software enables the preservation of important information from exploration to production. This, keeping the reservoir model updated to have a close vision of the subsurface, allowing the uncertainty analysis studio and the testing of multiple parameters and scenarios for sensitivity analysis through optimization workflows (Schlumberger, 2017b).

### **4.2. INTERSECT**

INTERSECT is a high-resolution reservoir simulator that allows the analysis of the flow of oil, gas, and water through the porous media. The user can set an initial solution as a function of pressure, the composition of each fluid phase present in the reservoir and saturation. This simulator will then provide the solution forward in time. The principle in the software is based in the conservation of mass by solving mathematical equations which allow concluding that the fluid phases are in thermodynamic equilibrium. Fluid and rock properties supplied by the user are presented in the equations mentioned previously. INTERSECT simulator was created to model more complex reservoirs and use of partition into regions, with their own properties and grid refinement levels, without any significant impact on the performance. Selection of this computational tool was mainly focused in the ability to run high-resolution models and local grid refinements, reducing run time simulations due to better parallel performance over ECLIPSE (Schlumberger, 2017a).

## 5. LOGGING WHILE DRILLING (LWD)

New technologies have been introduced over the years, especially with the emergence of new challenges in exploration and drilling of complex path lines wells. Logging while drilling is one of those technologies, characterized by the measurement of properties during the deepening of the borehole, using tools that are integrated into the bottom hole assembly (BHA). It has the advantage of measuring properties in real time and before the formation is invaded by drilling fluids. Guiding of the well placement can be done, in order to maintain it within the zone of major interest. Additionally, in highly deviated wells this technology is applied when wireline tools are very difficult to be run (Griffiths, 2009).

Other several benefits involved with logging in real time are (David Allen, 1989):

- Guaranteed data recovering, even if the well is lost.
- Real-time location of casing and coring points. Reduction in the uncertainty about potential bad hole conditions.
- Accurate location of the seismic reflectors during drilling. Enhancing stratigraphic mapping and well to well correlations.
- Faster recognition of potential zones, especially in the case of gas targets.
- $R_t$  determination while invasion is taking place.

### 5.1. Overcoming limitations in Horizontal Drilling

One of the limitations in conventional horizontal drilling is steering efficiently. Usually, the well is steered geometrically along the predetermined well path based on nearby well data and geological assumptions. Steering is mainly on bit direction and inclination data. In the case of resistivity and gamma ray measurements, a prudent distance far from the bit has to be taken into account and it is used just retrospectively. This practice is accepted as long as the target is thick and the structure is simple and well known. But, when the target is thin and the structure quite complex with lack of information to do a well-structured well planning other techniques start to play the main role. With advances in three dimensional seismic, operators are locating more complicated reservoirs and drilling more intricate wells. Current challenges embrace thin beds and folded or faulted reservoirs.

In the last cases, sensors located in the drill collars allow to replace the basic geometric steering for more effective geologic steering, or “geosteering”, which is the navigation of the bit using real-time information about the rock and fluid properties. A core application of this

technology is in the North Sea, where LWD is applied for geosteering and formation evaluation (Bonner et al., 1993).

In the case of the logs used for this specific project the tool run to obtain the petrophysical information was the EcoScope, which is a multifunctional design developed by Schlumberger, that integrates the study of formation evaluation, well placement, and drilling optimization measurements in the same run (Griffiths, 2010).

## 5.2. Petrophysics fundamentals

One of the main objectives of LWD is the reservoir evaluation of properties like lithology, porosity, saturation and permeability. Consequently, detailed information around the well is obtained and an optimization in the production can be assessed, updating the static model with new and accurate data.

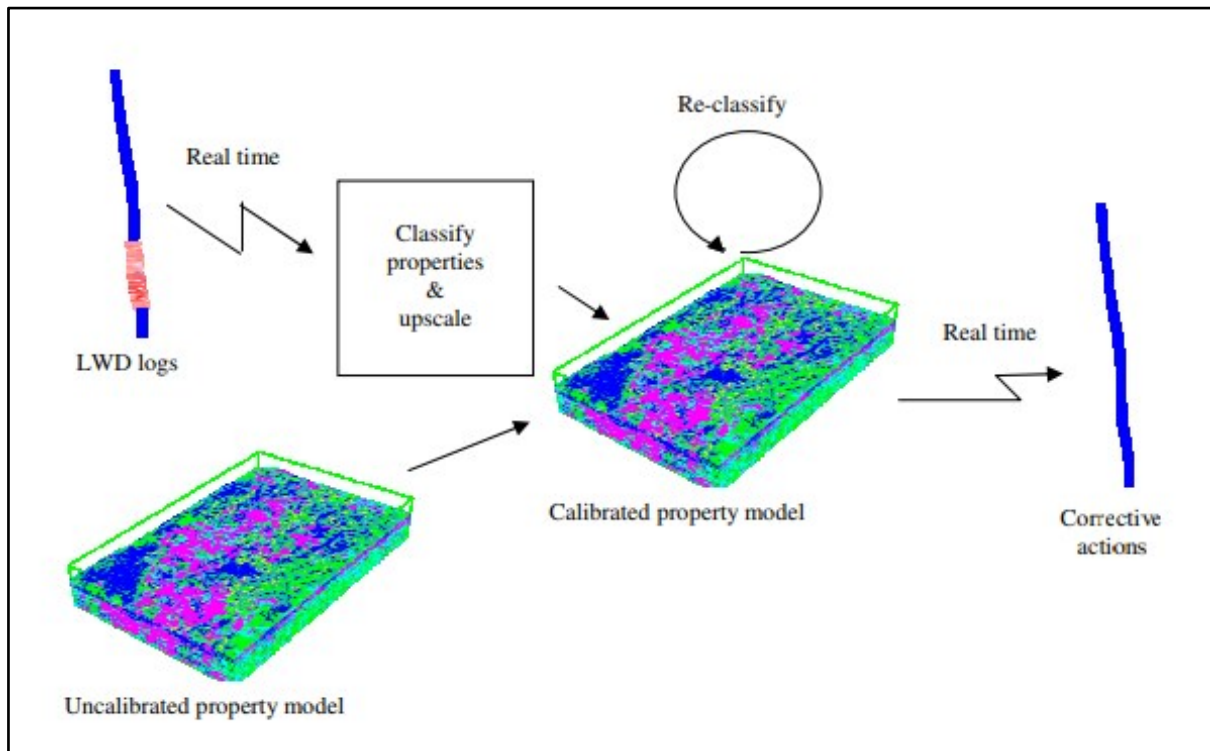


Figure 5-1 The uncalibrated model, created prior to drilling, is calibrated with the properties classified from the LWD logs as new measurement, example in geosteering applications, (Pedersen, Tennebo, Sonneland, & Carrillat, 2005).

For this explicit study, these are the evaluation methods for the following parameters:

### 5.2.1. Porosity Estimation

Total porosity is calculated using a total porosity model based on the density log where (Griffiths, 2009):

$$\phi_T = \frac{\rho_{ma} - \rho_B}{\rho_{ma} - \rho_{fl}}, \quad (5.1)$$

Where  $\rho_{ma}$  is matrix density,  $\rho_B$  bulk density and  $\rho_{fl}$  fluid density.

Matrix density is based on core measurements, bulk density is the density log (RHOB) and fluid density is calculated through iteration where the result is the apparent density formation, mud type and reservoir fluid.

### 5.2.2. Water Saturation

This property is calculated using Archie's equation, which allows the evaluation the formation water and hence the hydrocarbon saturation. The following equation is based on empirical correlation to experimental data (Archie, 1942):

$$S_w = \left( \frac{a \cdot R_w}{\phi_T^c \cdot R_{true}} \right)^{1/n}, \quad (5.2)$$

where  $a$  is tortuosity factor,  $c$  cementation exponent,  $n$  saturation exponent,  $R_w$  formation water resistivity (Ohm),  $R_{true}$  true -deep- resistivity (Ohm) and  $\phi_T$  total porosity (fraction).

### 5.2.3. Permeability Estimation

The prediction of the permeability is based on the multi-resolution graph-based clustering (MRGC), using logs derived from porosity and  $V_{sh}$  in order to calibrate the core permeability. MRGC is a multi-dimensional dot-pattern recognition method characterized for group data into small clusters which can describe the relationship between the input parameters in log space. As a general explanation, this method is characterized by a Neighboring Index (NI), Kernel Representation Index (KRI) and K Nearest Neighbor algorithm (KNN) which defines the neighboring connection of the data, the clusters they form and how the model is propagated to estimate permeability in the regions of interest.

This empirical method covers and improves the poor performance of previous methods caused by core-log depth mismatches and the occurrence of facies showing a strong dispersion of permeability due to heterogeneity at scale between logs and plugs (Ye & Rabiller, 2000).

## 6. CASE STUDY

This simulation case represents a sector model of an oil and gas reservoir located in the North Sea. Characterized by being a sandstone reservoir in the Brent formation, highly faulted and compartmentalized, the model was subdivided into 44 layers. The stratigraphic layering consists of the Upper Brent which contains the Tarbet and Ness formations, and the Lower Brent where Etive and Rannoch formations are present. The initial pressure of the compartment is 434 *bar* at datum depth of 2950 *m* and the water-oil contact is located at 2946 *m* depth.

In relation to the static properties, porosity distribution over the model is characterized to have medium to high values, which is typical of a fine to coarse grained-sandstone reservoir (Struijk & Green, 1991). Values oscillate between the range of 0.0081 and 0.3. The following graph illustrates the distribution of this property in the model.

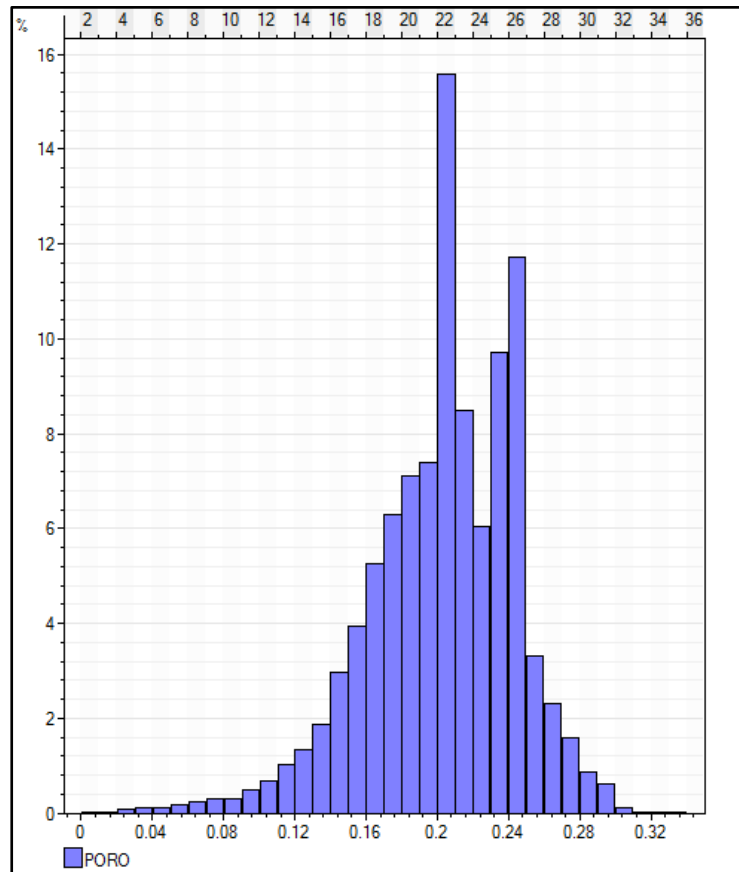


Figure 6-1 Histogram of porosity distribution in the reservoir model (Values in %).

In the case of the permeability, values in *i* and *j* directions are set equal and characterized to be between the range of 0 to 25000 *mD*. On the vertical direction, based in the anisotropy

concept the value of the permeability is a tenfold less than the horizontal permeability. The next figure shows the distribution in horizontal direction of the property.

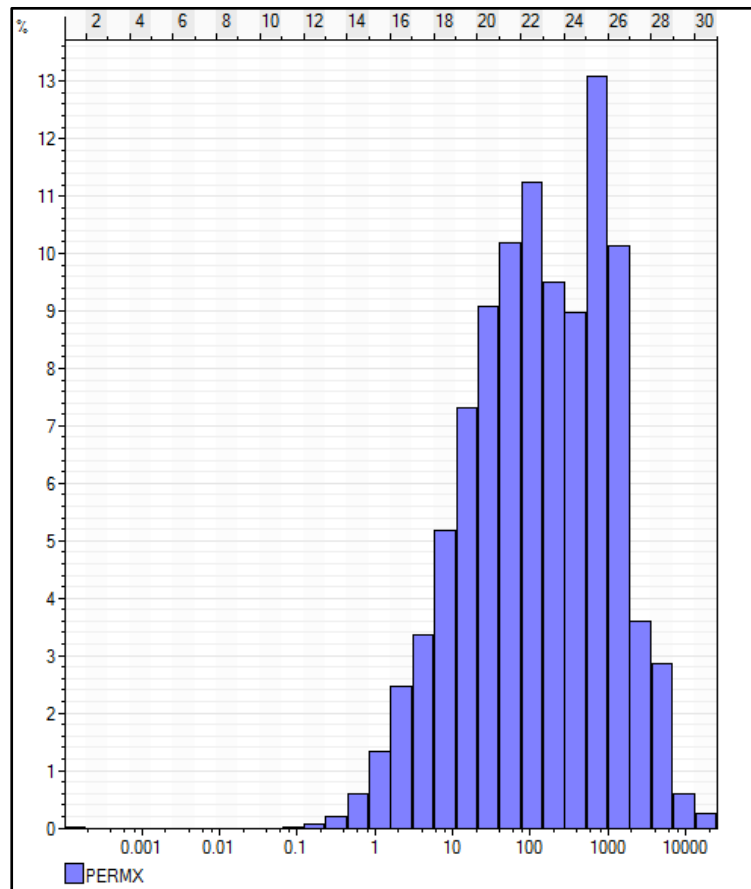


Figure 6-2 Histogram of horizontal permeability distribution in the reservoir model (Units in mD).

Currently, in the compartment dedicated to the study, there are two producer wells, one with perforations located in the Upper and Lower Brent, opened to production in March of 2000, while the second one, located in the Upper Brent, it was opened in October of 2016. The second one, is the main focus well of the present thesis. There is also one injector located in the compartment, opened in November 2010, which initially started injecting gas, followed by WAG (Water alternating gas) for a short period of time and finally only water. Perforations of this well are currently placed in the Upper and Lower Brent.

For a better understanding of the results, it has to be taken into consideration one of the previous producer wells that was open from 2000 to 2007. This well is referred as “old producer” in this thesis.

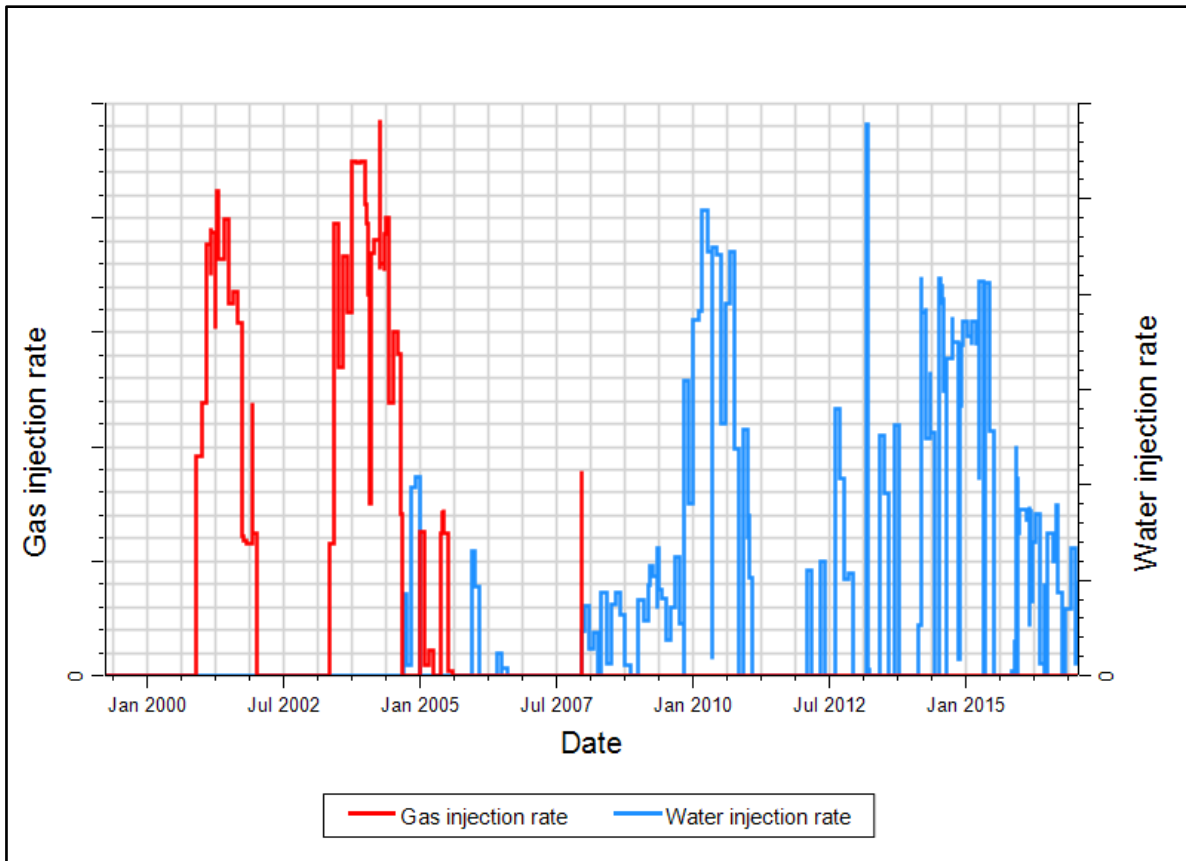


Figure 6-3 Sector model injection history.

### 6.1. High Angle Well (Producer well)

This producer well was planned to increase the oil recovery from the Upper Brent in the compartment. Initially, a different well path was drilled, but due to technical problems, a sidetrack was executed close to the first well path with some modifications associated with the optimization in the attack angle. The completion was simplified to cemented and perforated liner due to some complications during the drilling process. The well was open to production at the end of 2016. Four perforations intervals are present in this well as is illustrated in figure 6-4, but none of them located in the toe of the respective wellbore in order to avoid water production in an early stage. By the beginning of 2017, the well was producing oil and gas but did not show any indication of water breakthrough. This study is mainly focused on the influence of the injector over the high angle well when the properties nearby wellbore are changed using petrophysical data derived from real LWD log measurements. In the current project, each perforation intervals were designated with a number.

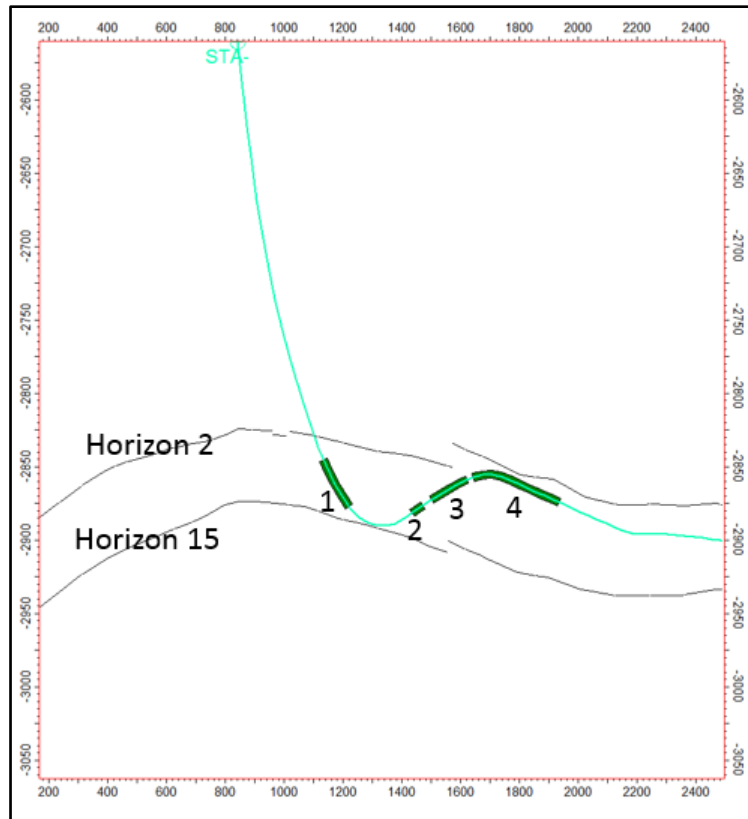


Figure 6-4 Location of the high angle well in the Upper Brent.

It is important to clarify that a fault is crossing from east to west direction of the compartment. The transmissibility values along the fault are characterized to be very low. Therefore, effects in the output dynamic properties are visible. This thesis will not cover the degree of transmissibility of the fault since this study is currently under development with the scope to build a new and more precise version of the model for further investigation.

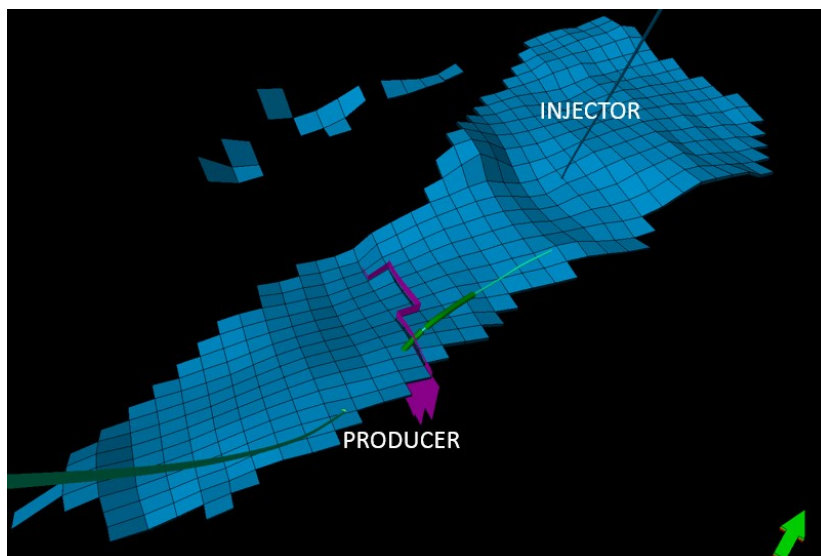


Figure 6-5 Fault crossing through the producer well.

## 7. METHODOLOGY

Data gathering was the first step done for the development of this study. Drilling reports, logging while-drilling records, information of the completions and production history were supplied by the client to have a realistic scenario for the sensitivity analysis.

Following this, improvements in the static model were done before running the simulations to study the impact of the updated properties in the sector model. In the end, prediction cases were created to compare the results against the Base case. The next sections show step by step the updates done in the sector model using Petrel E&P and INTERSECT.

### 7.1. Updating of the well completions

From drilling reports, a quality check and update of the completions were done for wells inside the sector model. This was carried out, with the primary purpose of studying the impact of the open perforations in the high angle well and the influence of the completion by adding a well segmentation to the simulation case. Likewise, the same process was applied to the other involved wells.

In the Well Engineering window from Petrel E&P, the manual design option is available in order to bring all the information of the wells into the static model. For each well, the completion type related with the presence of liners, perforations, plug and abandons, among others, was updated, as well as specifying the dates in which the items were made active and the sections where they were located.

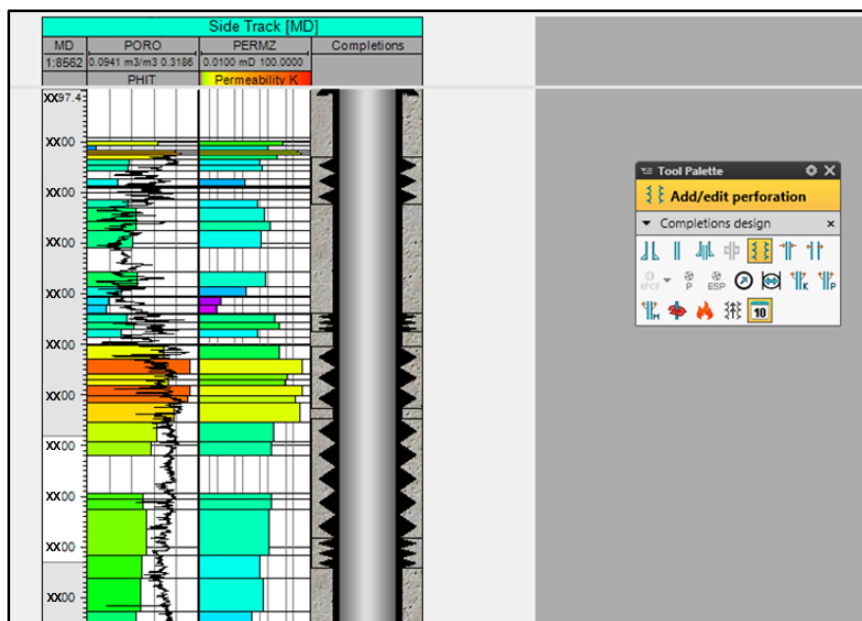


Figure 7-1 Completion design of the high angle well (producer well).

After completing this procedure, the following stage was to create a well segmentation which enables modeling of complex well topologies and multi-phase flow effects in the wellbore that was the case in this study. The well segmentation was created by, taking advantage of the tool available in the software. For the calculation of the pressure drop, friction and acceleration components were selected. The Appendix I displays in more detail the Completions manager and the Define well segmentation window established for this case.

### 7.2. Local grid refinement around the well

To study in a more detailed way the impacts of the updates of properties, a local grid refinement (LGR) was created around the producer well. The method to define the number of sub-divisions was Cartesian  $N_x, N_y, N_z$ . Extended host cells were along  $k$  direction and the source of influence was 100 m. In the following figure it is possible to appreciate the section of the sector model refined.

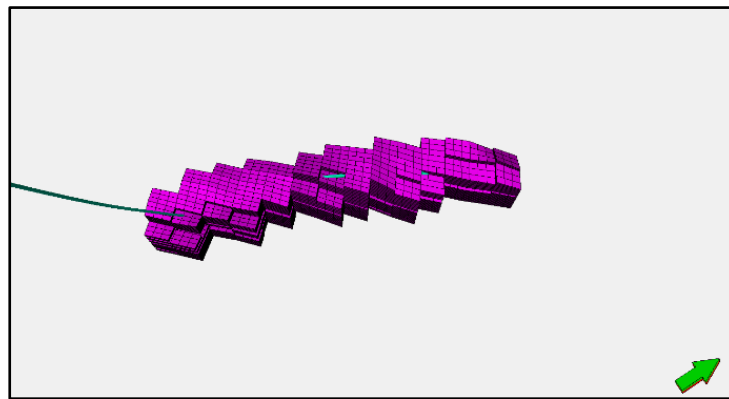


Figure 7-2 Local grid refinement around the producer well.

Considering the bulk volume of the sector model as  $154,536,466 \text{ m}^3$  and the one in the local grid as  $13,306,620 \text{ m}^3$ , this portion represents an 8.12% of the total compartment.

Once the respective LGR was set in place, the grid was then ready to continue with the property updating. For study purposes, this is the Base case selected for the sensitivity analysis.

### 7.3. Updating of the properties

This section is focused on the process of modification of the properties in the local grid using some software tools to populate the region in a more precise way.

With the purpose of ensuring a refinement of the properties inside the local grid taking into consideration the dimensions of the grid, a plug-in, which is an extra tool that can be added to

the software, was created. Using the Ocean framework, an extended platform for Petrel E&P, it was enabled to create and install the plug-in, which is characterized by having an input in order to get an output to be used in the current grid (Manchuk, Neufeld, & Deutsch, 2007). In this case, the input was the property refined considering the dimensions of the LGR, which is explained in more detail in the following subsection, and the output was the property populated only inside the local grid in the sector model after some calculator operations, leaving the rest with the initial property values. The next section explains in more detail how the properties were populated in the sector model.

### 7.3.1. Well log upscaling and petrophysical modeling

Porosity and permeability logs from wells located in the compartment were imported to Petrel. Based on the data presented in the model, a preliminary comparison was done just taking into consideration the logs of the producer well to evaluate the degree of difference in properties.

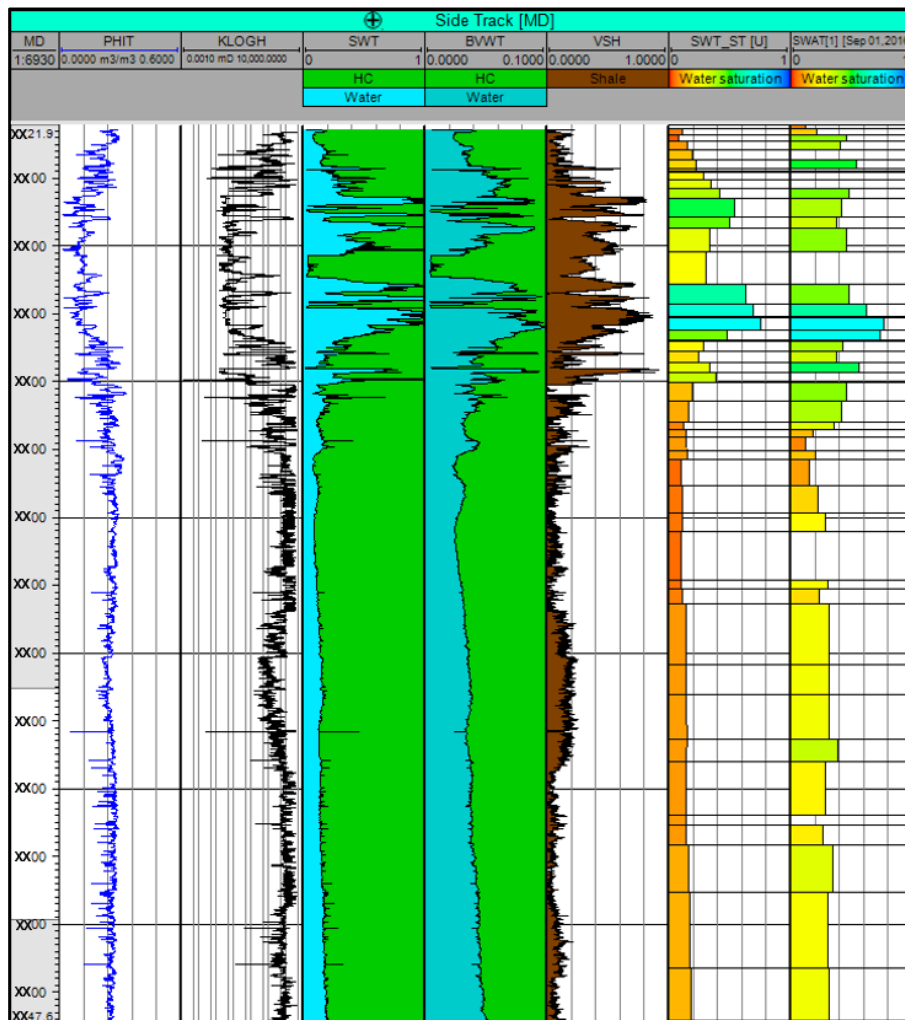


Figure 7-3 Producer well logs (Porosity, permeability, water saturation and volume of shale).

The first stage was the upscaling of logs. In the software, each grid cell takes a base log value and uses algorithms to produce one result. After the upscaling of the log, a simple comparison of the property values just in the cells that coincide with the trajectory of the well was done. Taking into account the values given by logs as the real ones, the total porosity varied between a decrease of 9% and an increase of 10% of the pre-refined model. For the permeability, the gap between the minimum and maximum difference was noticeable, the minimum difference was a reduction of  $-6.27 \text{ mD}$  and the maximum one was an increase of  $2124 \text{ mD}$ . It is important to clarify that the following update properties in the grid took into consideration multiple logs, which generated the final values of porosity and permeability.

Subsequently, the problem to solve was related to the refinement of the property using the same dimensions as the LGR. This, due to the fact that petrophysical modeling for local grids is not possible with the current version of Petrel, forcing to find another alternative to solve it. For this procedure, a copy of the principal grid was made in order to create a refinement with the same dimensions as the local grid. The upscaling step was repeated for the entire refined grid. The following step was to develop the petrophysical modeling, focused on property modeling, which enables to distribute the values in the model preserving the realistic reservoir heterogeneity and matching the well data. For this study, the modeling was based on the kriging interpolation, a deterministic model characterized by doing an estimation fully based on the parameter values given at the input step.

To complete the property population, the plug-in was used. This tool allowed to populate just the local grid with the property refined in the principal grid, used for the study. The workflow of the plug-in, as it was mentioned before, it is essentially input to output data processing.

The next graphs allow visualizing the final result obtained from the upscaling and petrophysical model for the porosity and permeability.

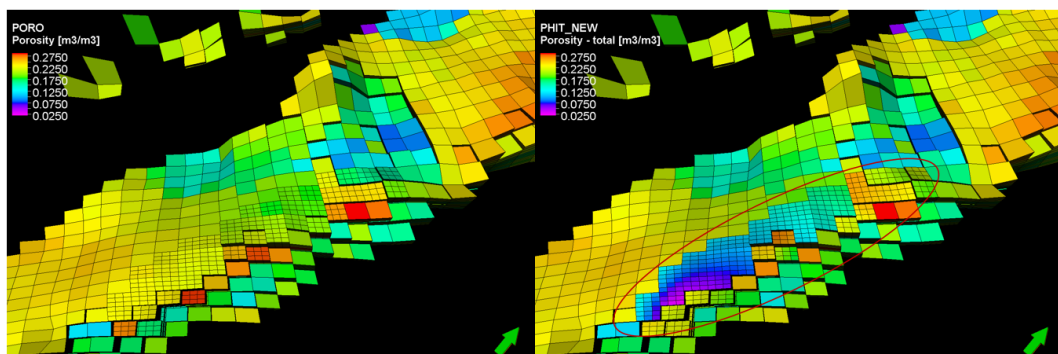


Figure 7-4 Porosity updates in the local grid (left: No updates, right: Porosity updates).

Regarding only the LGR, it depicts an overall mean porosity reduction of 11.79% in comparison with the original property values.

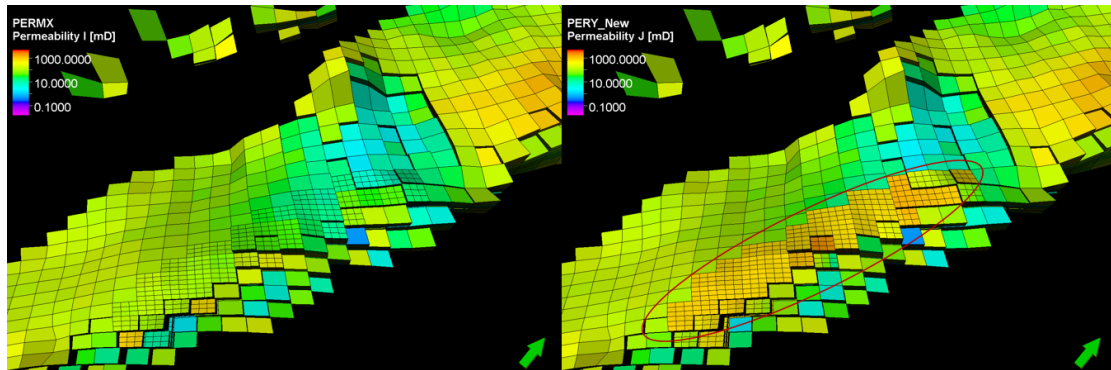


Figure 7-5 Permeability updates in *i* and *j* direction in the local grid (left: No updates, right: Permeability updates).

For the case of permeability, an evident increase in values was obtained. Comparing the mean horizontal permeability before and after the updates, there is a rise of 4 times the original values taking into account the data from the logs. Considering the extension of the local grid selected and the meaningful variation on the permeability values, the introduction of a significant contrast at the edge of the refined part is going to have an effect at the moment that the simulations are run.

From the sector model updated it will be interesting to understand the impact when these properties are changed in the selected zone on the behavior of the fluid flow from the injector towards the producer to predict the time of water breakthrough and decisions related with production optimization.

#### 7.4. Creation of the field management strategy prediction

A prediction case was created mainly focused on the production performance of the high angle producer well. This case was set up for a period of eight years, taking into consideration the neighboring compartments that could affect the pressure and production effects. Four more wells were added to the case and some group controls were established using the option named guide rate balance actions from the Field management strategies available in Petrel E&P for INTERSECT runs. Group controls are related with rates of injection and production for specific compartments. In the case of the producer and injection wells, the following tables show the rate and pressure controls set up for the individual wells.

Table 7-1 Rates and pressure controls in the producer well.

Oil production rate	150	sm <sup>3</sup> /d
Water production rate	500	sm <sup>3</sup> /d
Gas production rate	1500000	sm <sup>3</sup> /d
Production tubing head pressure	100	bar

Table 7-2 Rate and pressure control in the injection well.

Water injector rate	1500	sm <sup>3</sup> /d
Injector bottom hole pressure	600	bar

For the development of this forecast study, it was necessary to input some VFP tables (Hydraulic tables) with which it was possible to describe the well fluid model in the wellbore. These primary tables provide data of the relationship between the tubing head pressure (THP) and bottom-hole conditions in the well. Having this data, the INTERSECT can consider pressure changes in the tubing, wellbore and surface equipment.

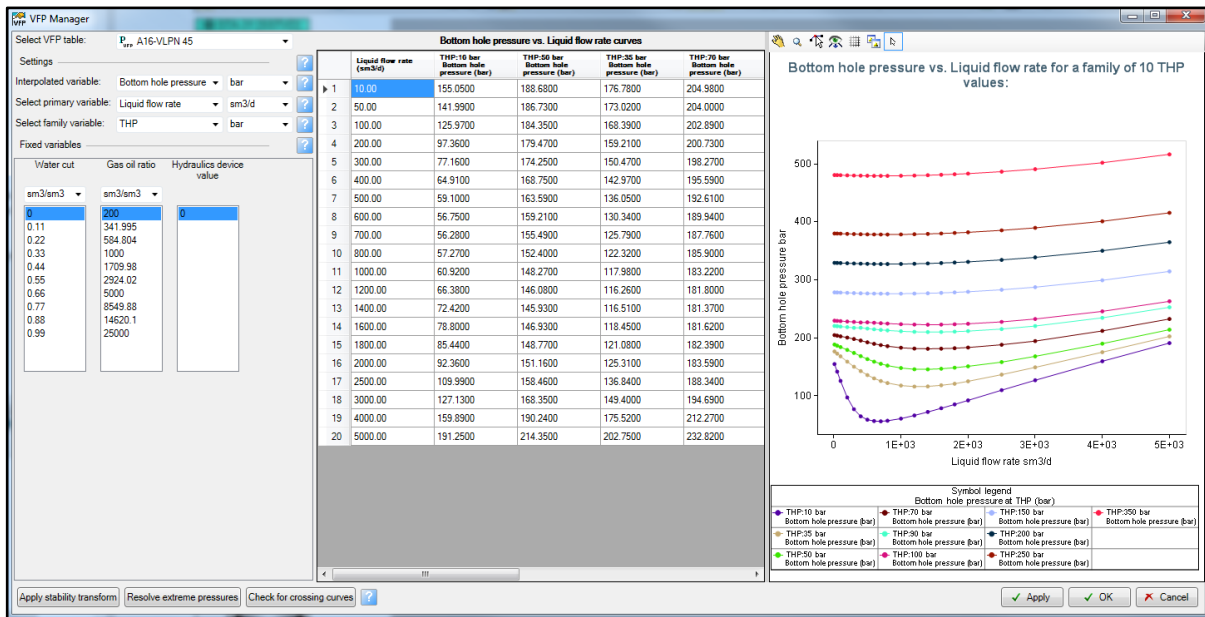


Figure 7-6 VFP (Hydraulic table) used in the prediction strategy for the producer well.

### 7.5. Set up of the prediction cases

With the prediction strategy established, the subsequent step was to select the simulations to run. Well segmentation for the wells and global permeability logs were added in each one of the simulation cases. Multiple cases were established to visualize the impacts on the properties

updating. It is important to clarify that for each prediction case, that the historical part was also re-run with the specific property updated. That is why, since the starting point of the prediction cases it is already possible to observe some differences in the dynamic results.

For the sensitivity analysis, the first property changed was the porosity, where simulation grid results like pore volume and production rates in the producer well showed the first impacts. The second updated property was the permeability, showing an interesting change in transmissibility values and the velocity in the water front from the injector to the producer. Finally, the impact when both properties are updated was studied.

Likewise, an additional case was run to evaluate how big the difference is when just a portion of the local grid is populated with the new properties. For this special case, a polygon was created inside the local grid using Polygon editing and some property calculations. The polygon was modified with the new property values while the rest of the local grid and sector model was populated with the base case properties. It is interesting to see the impacts of this cases in the results section.

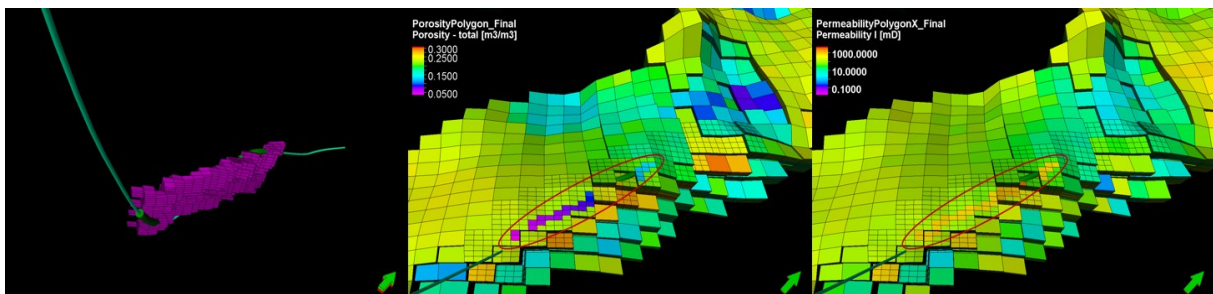


Figure 7-7 Porosity and permeability (*i* and *j* direction) updates inside the polygon.

Finally, the influence when some of the perforations are closed was studied. This was done to bring up some possible options of different completion designs for the producer well compared with the current one. For this exercise, the change was done by the completions manager, modifying the producer zones. The first prediction case was closing the perforation 1, while the second prediction was closing perforations 1 and 2. In both simulation cases, adjustments were done since the beginning of the production when both properties were modified. To see the changes in the water front behavior that reaches the producer well.

## 8. RESULTS

Simulations were performed using INTERSECT. The period of prediction goes from 2017 to 2025, with a monthly time step to evaluate the changes in properties. The following results are given taking the original properties and a local grid refinement around the well as a Base case and the properties updates as a sensitivity test of the model in order to see the impacts of the updates from logging while-drilling data.

Effects of the change of properties will be shown in this chapter, followed by a sensitivity study of the extent of the area that was populated to compare the general effect of the updates. Lastly, an analysis of the perforations is developed to describe possible adjustments that could be done in the well plan as a result of the data modified.

Results display the variation in output properties since the first year of production (1999) to visualize the changes during the forecasting in the sector model, considering that the modifications were done at time 0 of the historic case.

### 8.1. Sector model with gridding refinement (Base case)

For the Base case, in which a local grid refinement is introduced around the well, the following graphs display the influence of the grid modification in the model.

#### 8.1.1. Field performance

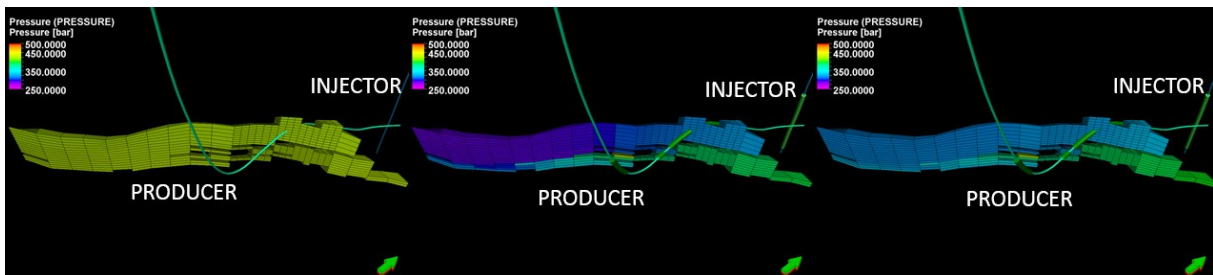


Figure 8-1 Dynamic pressure behavior in the sector model with local grid refinement in  $j$  direction (years 1999, 2017 and 2025)

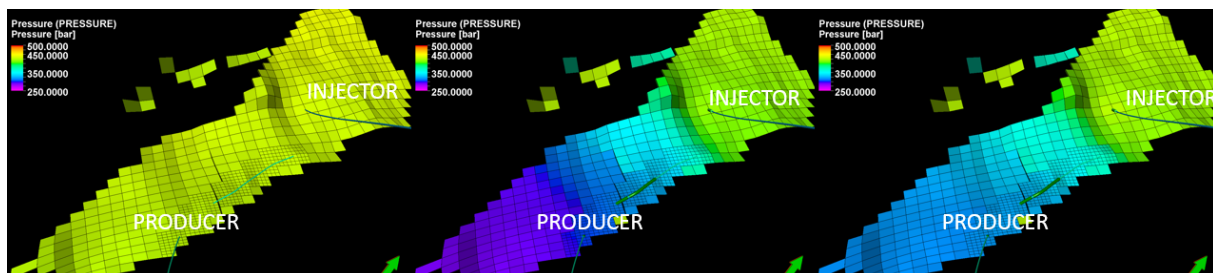


Figure 8-2 Dynamic pressure behavior in the sector model with LGR in  $k$  direction, layer number 5 (years 1999, 2017 and 2025).

Figure 8-1 and Figure 8-2 illustrate the behavior of the pressure in  $j$  and  $k$  direction, starting in 1999 until the end of the prediction. The area around the injector shows an increase in this property during the forecasting, which also is visible in the lower layers from Figure 8-1. An explanation to this increase can be the values of transmissibility in the zone around the injection well which helps to keep the pressure. In the case of lower layers, the reason can be the water injection at the bottom that helps to support pressure. The contrast in values between some layers in  $j$  direction is attributed to the existence of shales. It is important to mention that the presence of the fault shown in the subsection 6.1, has also an impact on the contrast between the north and south part of the compartment. The south part of the compartment shows an increase in the pressure which can also be attributed to the total volume injected, which is slightly higher than the total volume produced.

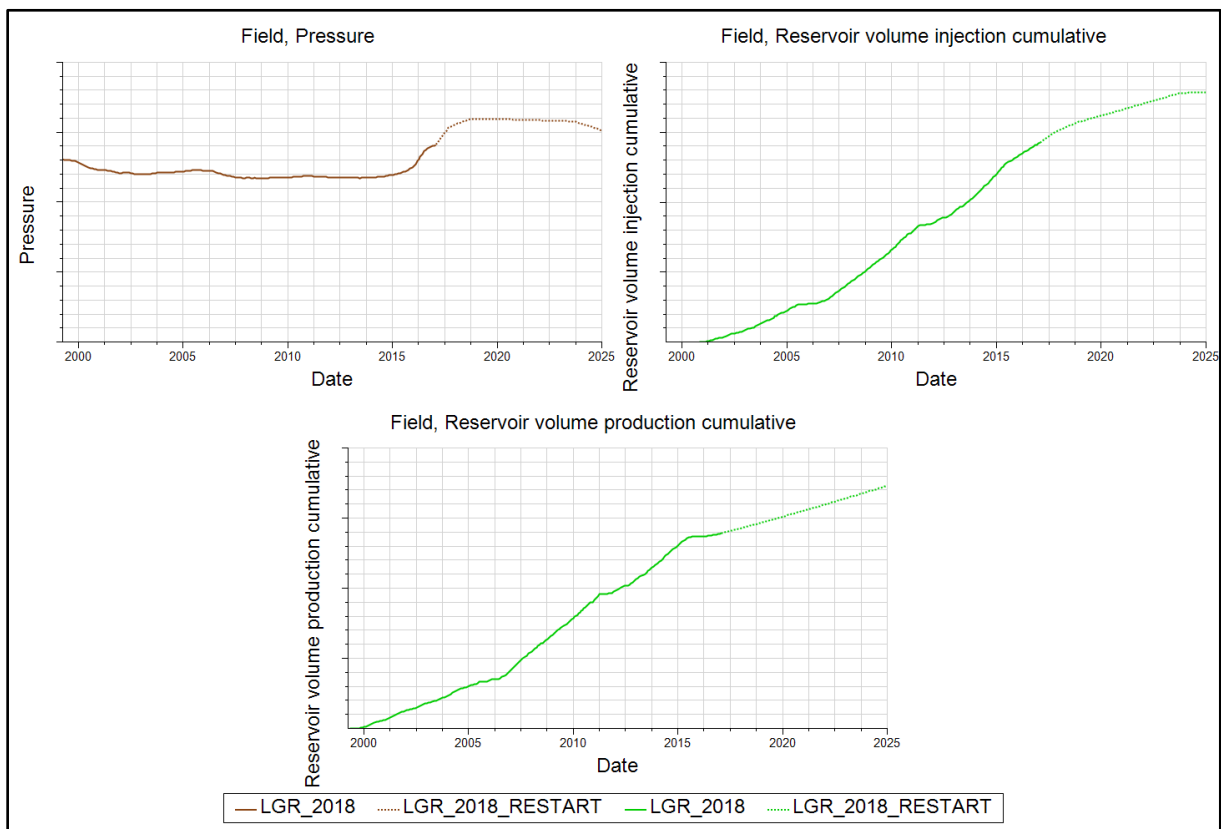


Figure 8-3 Field pressure and, cumulative injection and production for the Base case.

### 8.1.1. Bottom hole pressure and production rates in the producer

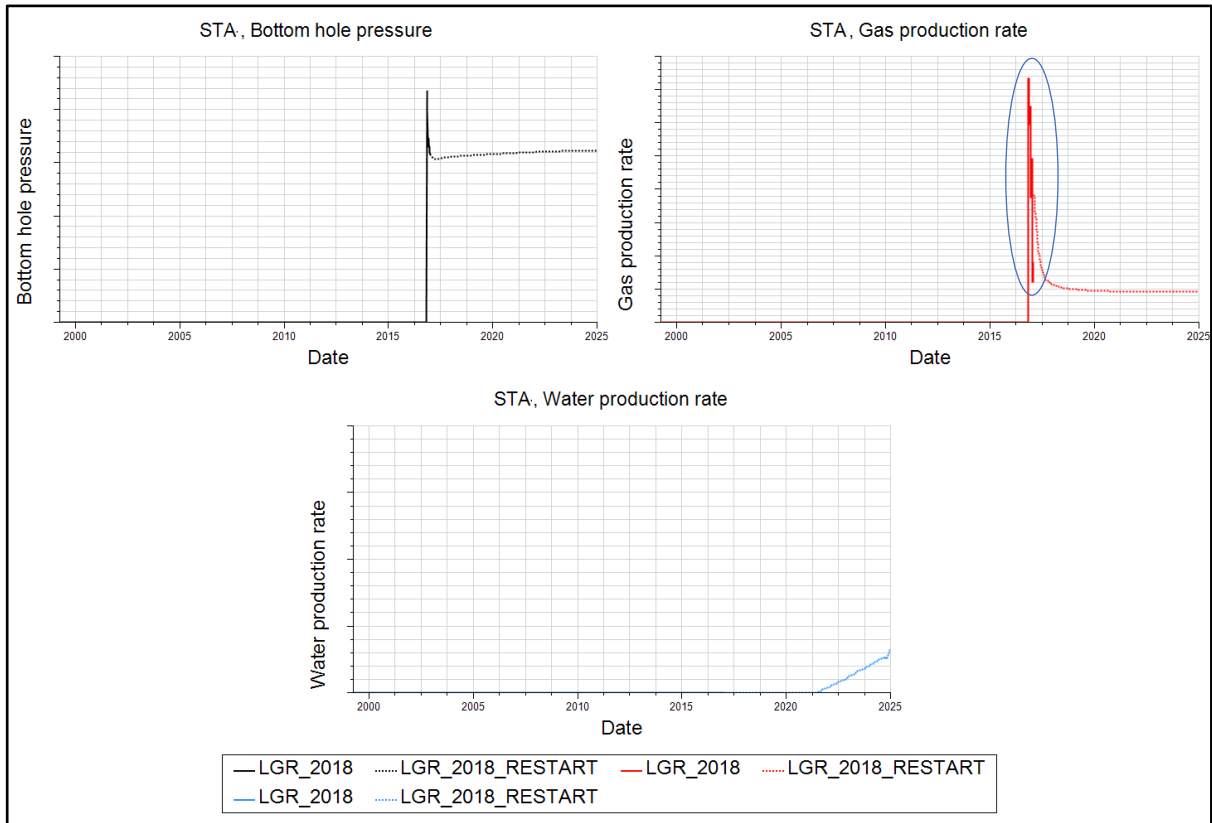


Figure 8-4 Production rates in the high angle well (historical and prediction case).

Figure 8-4 shows the historical and prediction cases for the producer well located in the sector model with LGR. As mentioned before, the oil production rate was set up as a constraint in the Field management strategy for this study. The water breakthrough is expected approximately in February 2021. The reason for the initial production of gas in the study well will be explained in the following subsection.

### 8.1.2. Influence of the saturation of gas on the producer well prediction since start-up of production

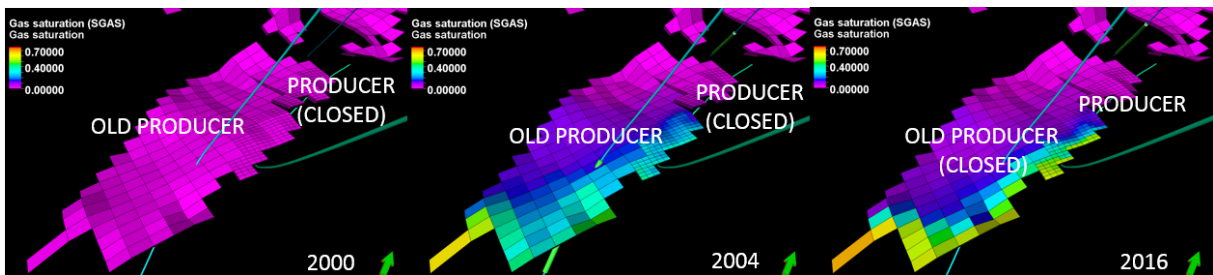


Figure 8-5 Saturation of gas in the historical case (k direction)

Figure 8-5 shows the saturation of gas due to the production of a previous well active from 2000 until 2007 (old producer) in the historical case, which can explain from where the initial production of gas in the high angle well is coming (Figure 8-4).

### 8.1.3. Water Saturation changes

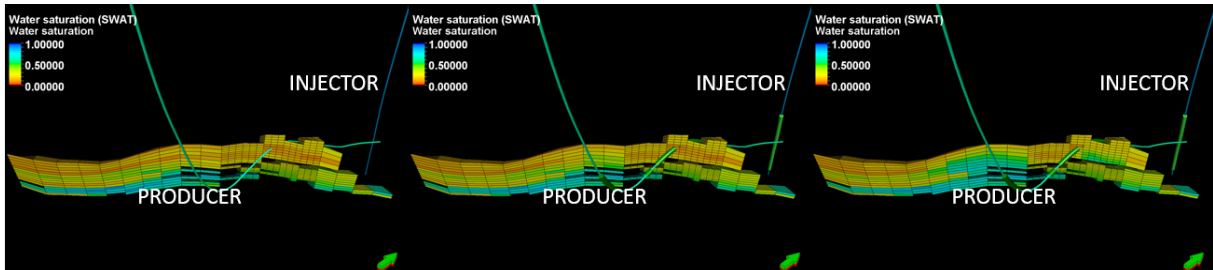


Figure 8-6 Water saturation changes in j direction in the Base case model (years 1999, 2017 and 2025)

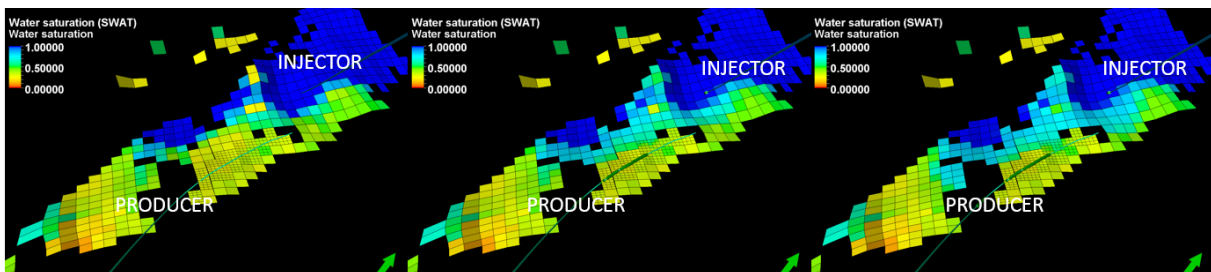


Figure 8-7 Water saturation changes in the Base case model for the years 1999, 2017 and 2025 (layer 8, k direction).

The Figure 8-6 and Figure 8-7 above show changes in saturation of water at the time 0 of production and at the beginning and end of prediction. The water front is approaching mainly from the injector to the toe of the producer during the forecast. This behavior is attributable to the heterogeneity in the properties present in the sector model, which implies that the water predominantly flows through high permeability zones in which it is easier to move.

### 8.2. Sector model with LGR and porosity updates (Case 1)

This section is mainly devoted to the impacts when just porosity was changed in the local grid around the producer well:

### 8.2.1. Pore volume changes

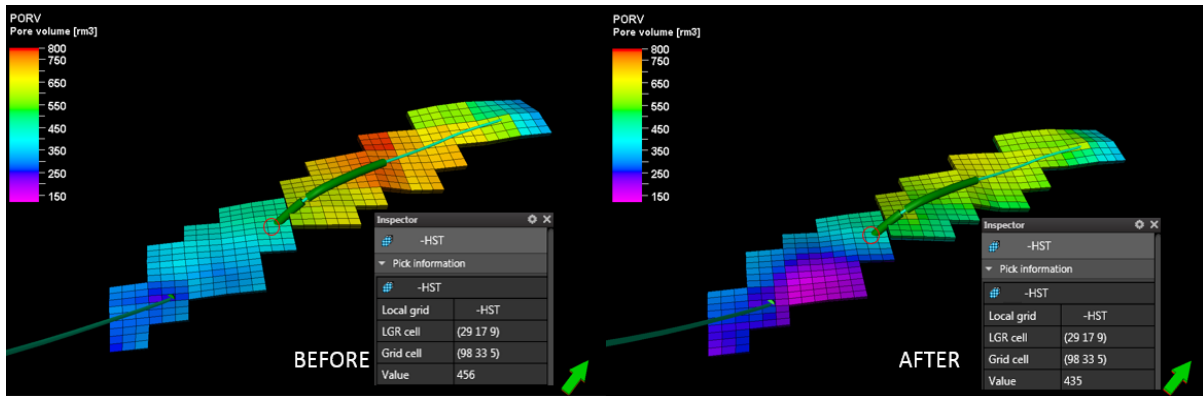


Figure 8-8 Pore volume before and after the update of the property (layer number 5).

A decrease in pore volume values is appreciated after the modification of the property around the producer well. As an example, the LGR cell (29 17 9) which is touched by the well, was selected in order to see the impact on the property modification. Originally the pore volume was  $456 \text{ m}^3$  and after the modification, the value obtained was  $435 \text{ m}^3$ , a reduction of around 4.6%. Applying a filter in layer number 5 (Figure 8-8), it is possible to determine easily the impact of the updates, for the local grid without and with changes in this property. The minimum and maximum values are shown in the following table:

Table 8-1 Pore volume changes in layer number 5 (k direction)

	Min	Max
Base Case	$243 \text{ m}^3$	$797 \text{ m}^3$
Case 1	$128 \text{ m}^3$	$661 \text{ m}^3$

Considering the mean values of pore volume before and after the property modification in the entire LGR the percentage of change was 13.14%.

### 8.2.2. Field performance

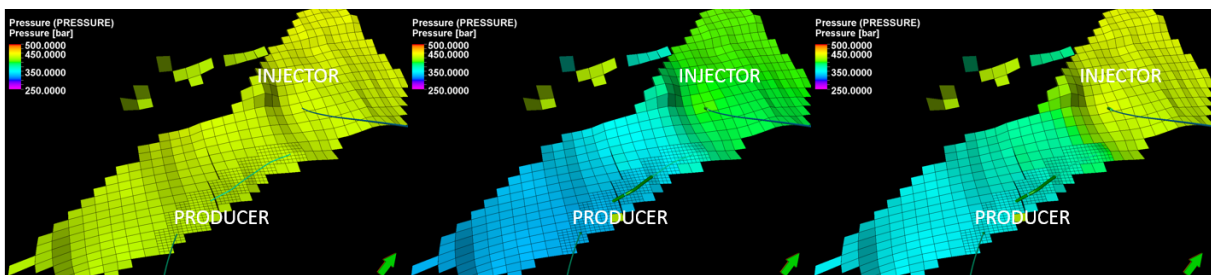


Figure 8-9 Dynamic pressure behavior in the sector model at the years 1999, 2017 and 2025.

Porosity updates generate a difference in the pressure behavior with respect to the Base case (Figure 8-1). Considering the reduction of the pore volume and the injection of the same amount of volume that in the Base case, a pressure increase in the compartment is produced which respect to the previous case during the forecast.

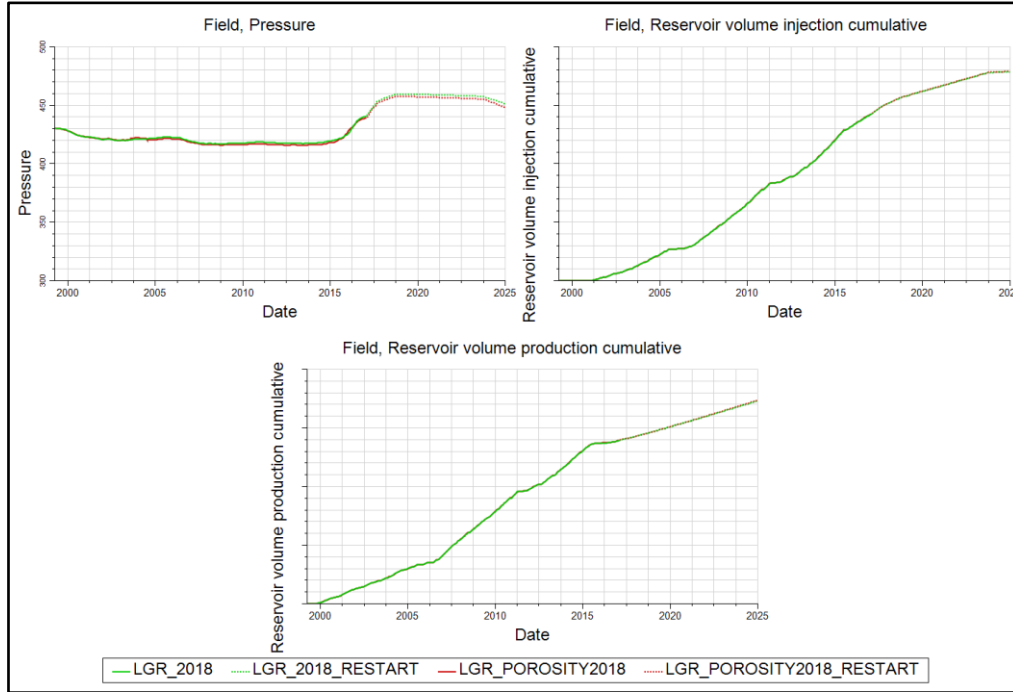


Figure 8-10 Field pressure and, cumulative injection and production for the Base case and Case 1.

### 8.2.3. Bottom hole pressure and production rates in the producer

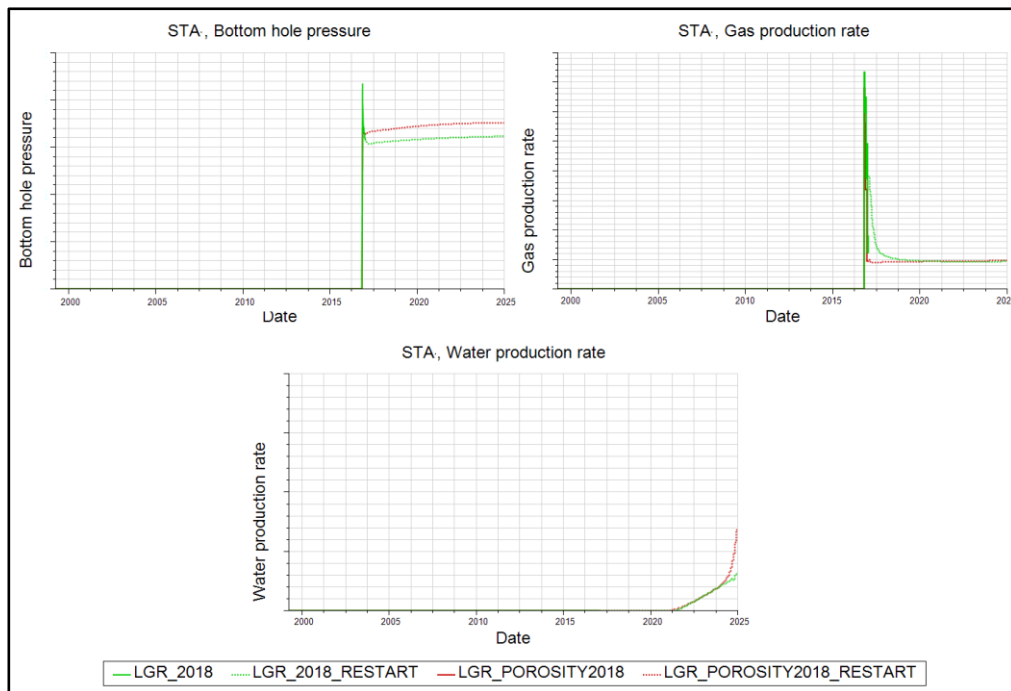


Figure 8-11 Bottom hole pressure and production rates in the high angle well considering porosity updates.

From 2025 (Figure 8-11), prediction of the bottom hole pressure, gas, oil, and water production are shown without and with porosity updates. The bottom hole pressure for the Case 1 shows an increase of approximately 20 *bar* when the prediction initiates. In the case of the gas, production is attributed to the free gas present near to the producer well. For the current case, with porosity updates, the water front comes just two months before, which is not visible in the respective figure. By the end of the prediction, the bottom hole pressure depicts a decrease.

#### 8.2.4. Difference in water saturation ( $dS_w$ ) at the beginning of the prediction

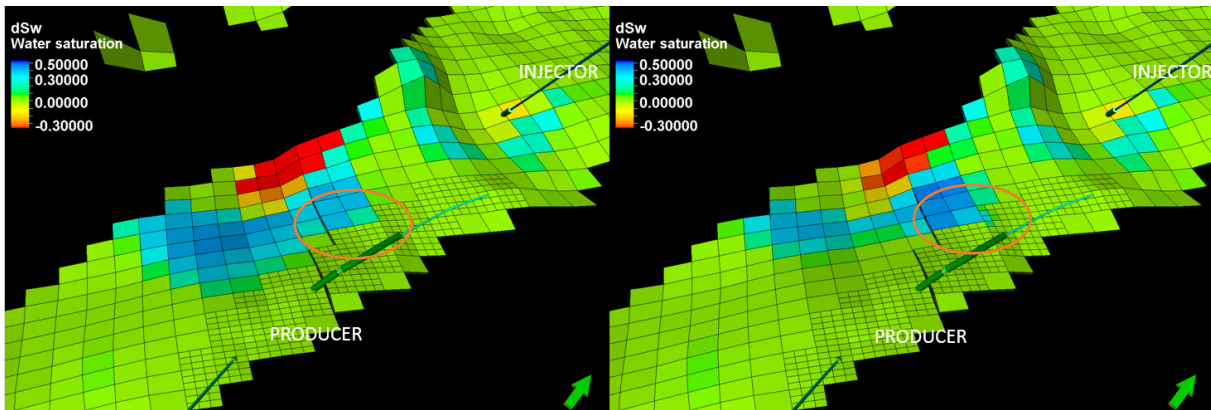


Figure 8-12  $dS_w$  before and after property modifications (Base case and Case 1 respectively at the end of the historical case, beginning of the forecasting).

Reduction in porosity anticipates the water front just a few months with respect to the Base case. The Figure 8-12 shows which cells of the LGR have a noticeable  $dS_w$  ( $S_w - S_{w0}$ ) at the beginning of the prediction case, for the Base case on the left side and the updated case on the right one (Case 1). From the illustrations, it is possible to see that at the beginning of the prediction the saturation of water tends to change near to the last perforations, which trigger a change in relative permeability ( $K_r$ ) to the water. Consequently, the  $K_{rw}$  is bigger and it moves faster, which can generate an earlier WBT. An example is shown in the following graph in which a comparison in the water saturation ( $S_w$ ) at the beginning of the prediction is presented:

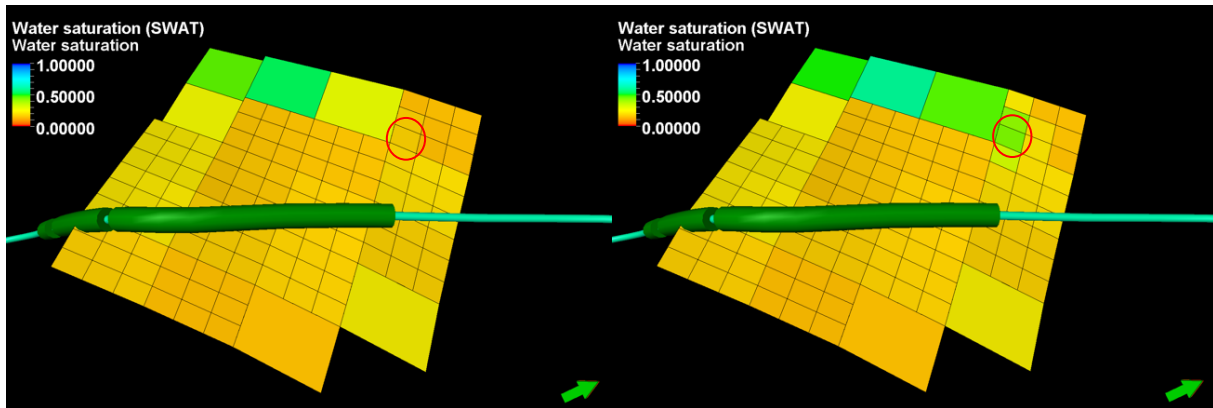


Figure 8-13 Comparison of  $S_w$  in the Base case (left) and Case 1 (right) in 2025.

LGR cell (94 29 5) was selected to compare this impact.  $S_w$  in the cell of the Base case model is 0.17 with represents a  $K_{rw}$  of approximately 0.001, while in Case 1, the  $S_w$  is 0.44, which represents a  $K_{rw}$  of 0.066 (see Appendix III).

### 8.3. Sector model with LGR and permeability updates (Case 2)

The same procedure was developed with the permeability to analyze the influence individually. It was considered the anisotropy convention for the vertical permeability as it was mentioned in Chapter 6. The following sections display the major impacts related to the change in this property.

#### 8.3.1. Permeability variations in the LGR

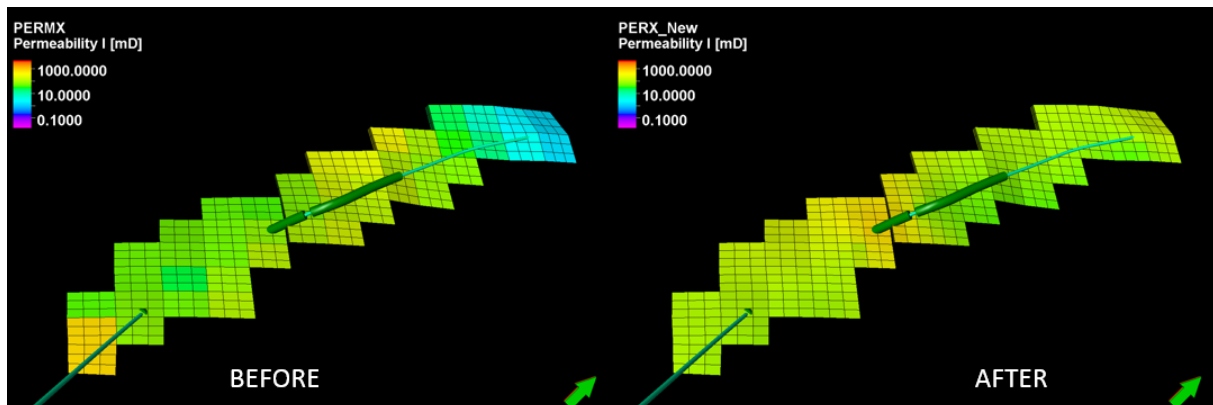


Figure 8-14 Permeability  $i$  direction (layer number 5 of the LGR).

Figure 8-14 illustrates the change of permeability for layer number 5 in  $i$  ( $x$ ) and  $j$  ( $y$ ) direction of the local grid, considering that these values are the same. Variations in permeability affects the flow fluid path, that is why, a comparison was done before and after this update. The mean

values for the zone selected changes from 121.19  $mD$  to 263.36  $mD$ , which generated an increment of about 54% in this property.

### 8.3.2. Field performance

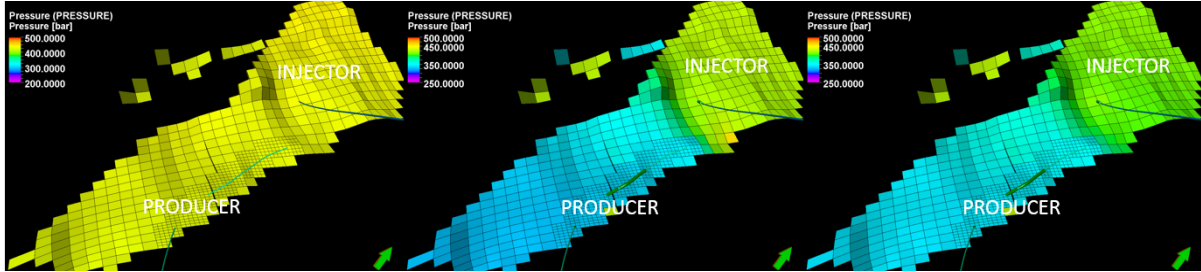


Figure 8-15 Dynamic pressure changes at the starting of the production, beginning and ending of the forecasting (1999, 2017 and 2025 respectively)

Considering the increase in permeability values, pressure showed a decrease with respect to Case 1 at the end of the forecast. As in the previous cases, the total volume injected still slightly higher than the total volume produced, explaining the increase in values of the pressure.

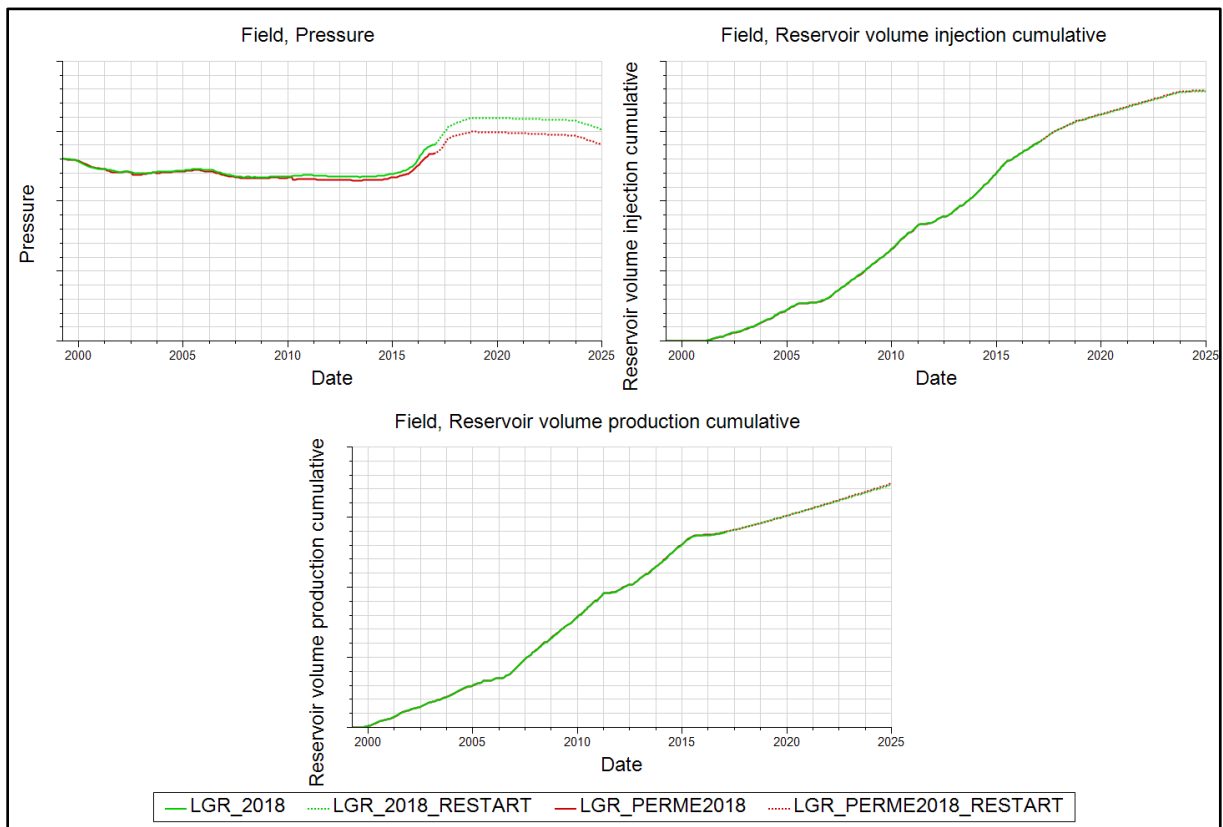


Figure 8-16 Field pressure and, cumulative injection and production for the Base case and Case 2.

### 8.3.3. Bottom hole pressure and production rates in the producer

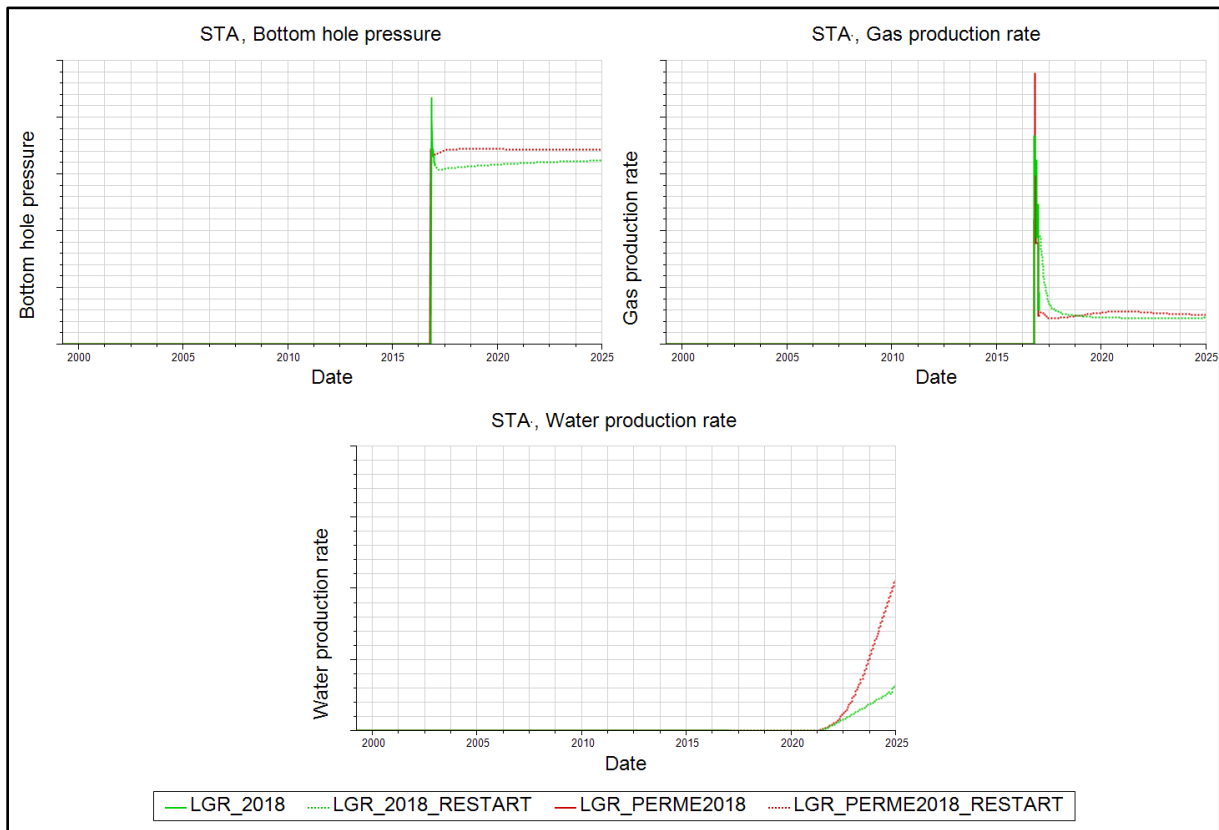


Figure 8-17 Bottom hole pressure and production rates in the high angle well with permeability updates.

Charts for bottom hole pressure and reservoir volume production for gas and water are presented (Figure 8-17) for the producer well. In the case of the bottom hole pressure, when the permeability was updated, an initial increase of around 26 *bar* continuing with a slight decrease can be appreciated during the prediction. The increment of the reservoir pressure also implies that the BHP increases, regardless of the increment in the production of water and the subsequent decrease in the relative permeability to the oil ( $K_{r_o}$ ). The increase in permeability makes the water front arrive just one month earlier at the producer well, but production values are more significant during the time. Initial gas production is much higher than in the previous cases due to the increase in permeability. Followed by the dissolved gas production.

### 8.3.4. Water front behavior

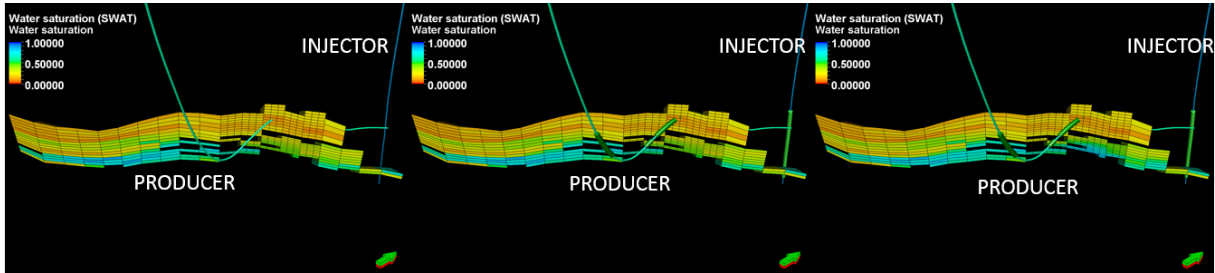


Figure 8-18 Water displacement in the prediction case for the years 1999, 2017 and 2025 (j direction).

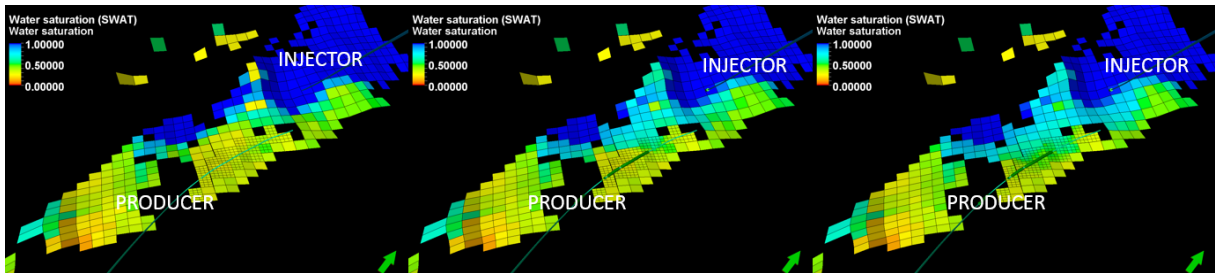


Figure 8-19 Water front behavior in the Case 2 for the years 1999, 2017 and 2025 (layer 8, k direction).

Changes in permeability accelerate the water front of the producer well with respect to the Base case (Figure 8-7). The images illustrate the displacement of the water when the production starts and during the prediction. Water moves from the injector to the north of the producer. In Figure 8-18 it is possible to appreciate how the water front is moving from a lateral view.

### 8.4. Sector model with LGR and porosity and permeability updates (Case 3)

After studying the impact of the properties individually, the following sections illustrate the change in the production and water breakthrough when both porosity and permeability are updated to have a more precise representation of the reservoir considering that this data was obtained from the logs.

#### 8.4.1. Field performance

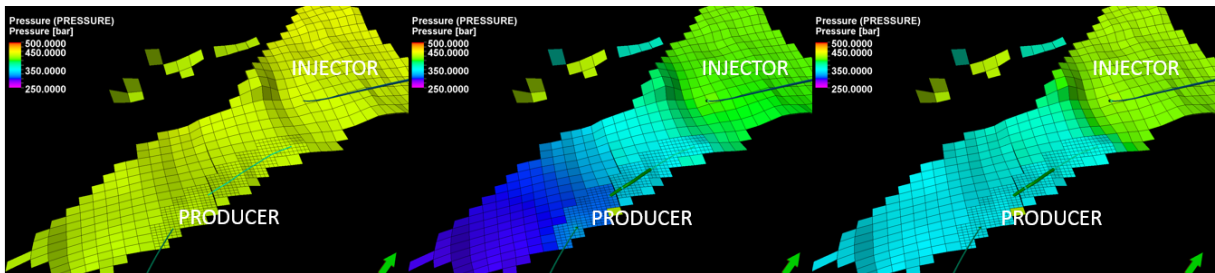


Figure 8-20 Distribution of dynamic pressure at the beginning of the production and during the prediction time (1999, 2015 and 2017 correspondingly).

Figure 8-20 illustrates the final effect when both properties are modified. As is expected, values in the pressure are between Case 1 and Case 2 at the end of the prediction.

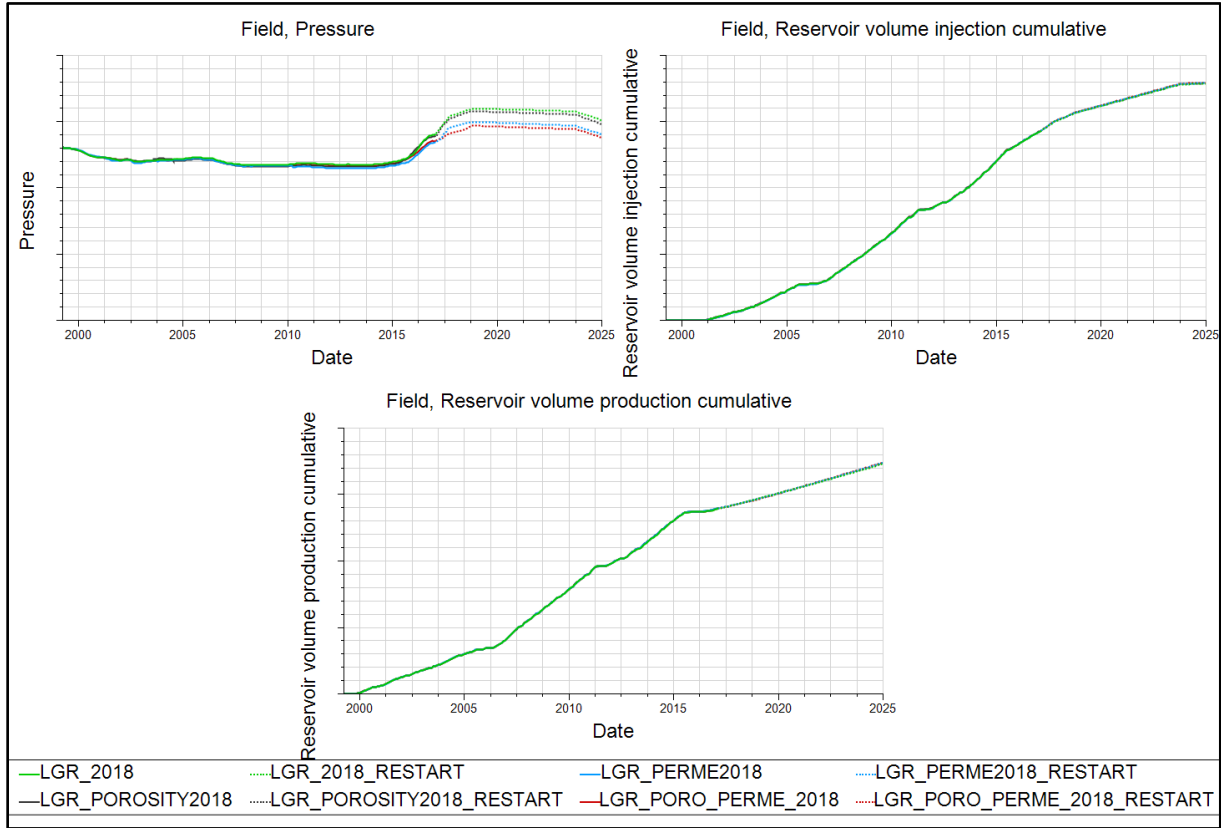


Figure 8-21 Field pressure and, cumulative injection and production for the Base case and Case 3.

Values of volume injection still being higher than the values of produced volume. The effect of the added properties generates a higher depletion in the field that is shown the Figure 8-21, comparing the reservoir pressure from Base case with Case 3.

### 8.4.2. Bottom hole pressure and production rates in the producer

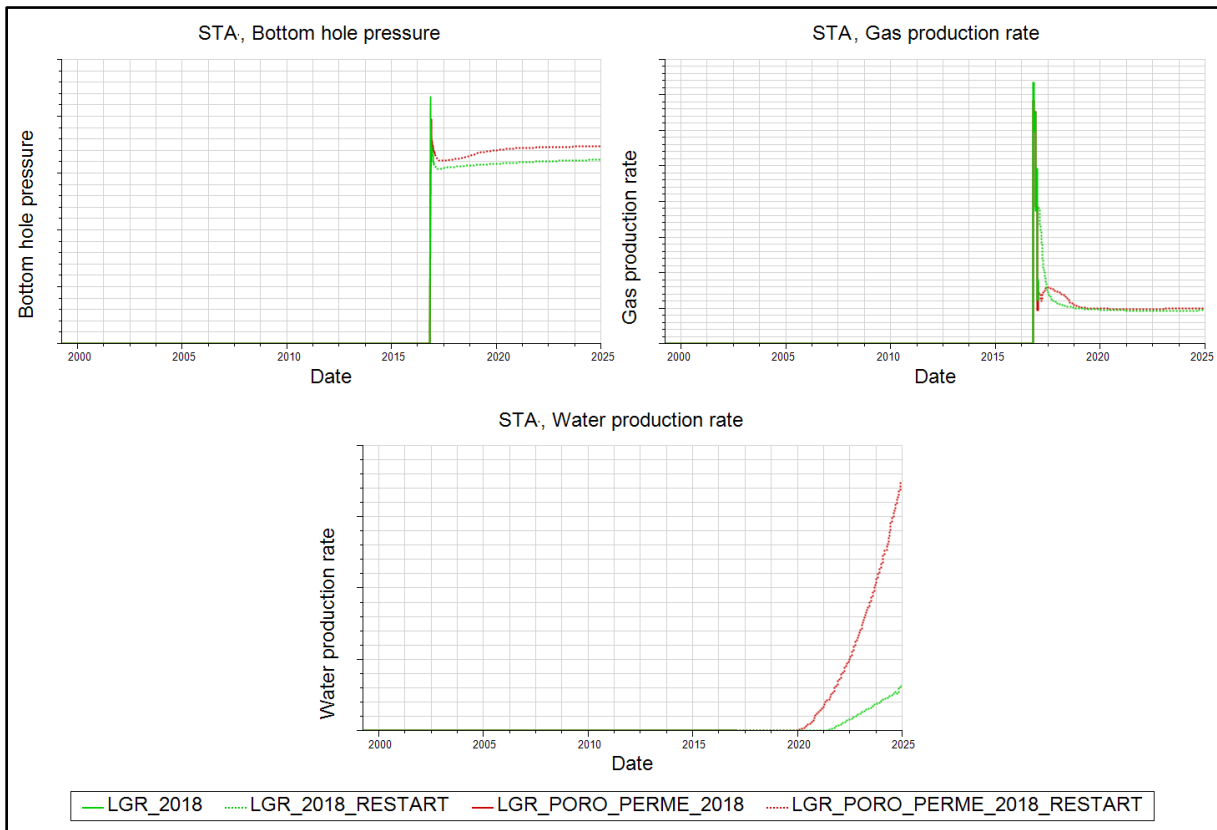


Figure 8-22 Bottom hole pressure and production rates in the high angle well, Base case and with property updates (Case 3).

In this case (Figure 8-22), it is possible to visualize that the water breakthrough reaches the producer well almost a year and a half before that when the LGR has not property updates. Following the results when each one of the properties was updated, Case 3 is consistent considering the impact on the WBT when porosity and permeability are added simultaneously. For the gas, the production is minor when this starts in comparison with the Base case and it remains constant over time, which means that the gas is not being released from the oil at reservoir conditions.

### 8.4.3. Water saturation changes

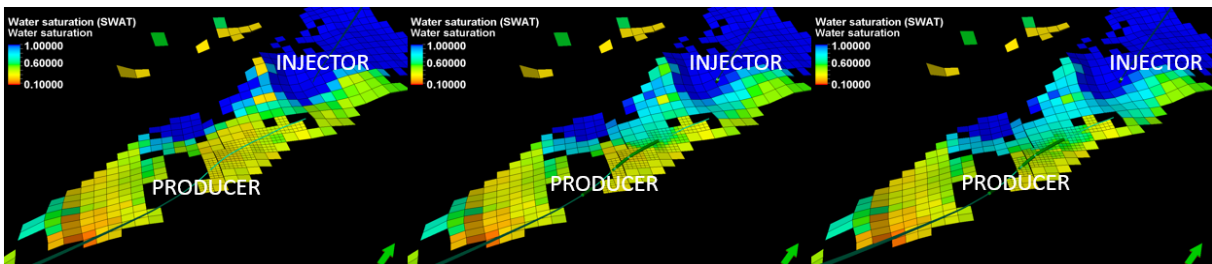


Figure 8-23 Water saturation changes in the Case 3 for the years 1999, 2017 and 2025 (layer 8, k direction).

The water front presents a similar behavior to Case 2 (see Figure 8-19). In this case, the flow path is controlled by the sum of the impacts related to the increase in permeability and decrease in pore volume. The front velocity increase towards to the producer well with respect to the Base case and the propagation of the water front is more significant in the north area, towards the producer.

#### 8.4.4. Water flow rates in each perforation

The following figures describe the water flow from each one of the segments associated with the four perforations. The purpose was to study possible different configurations for the producer well considering the predicted water breakthrough in each perforation.

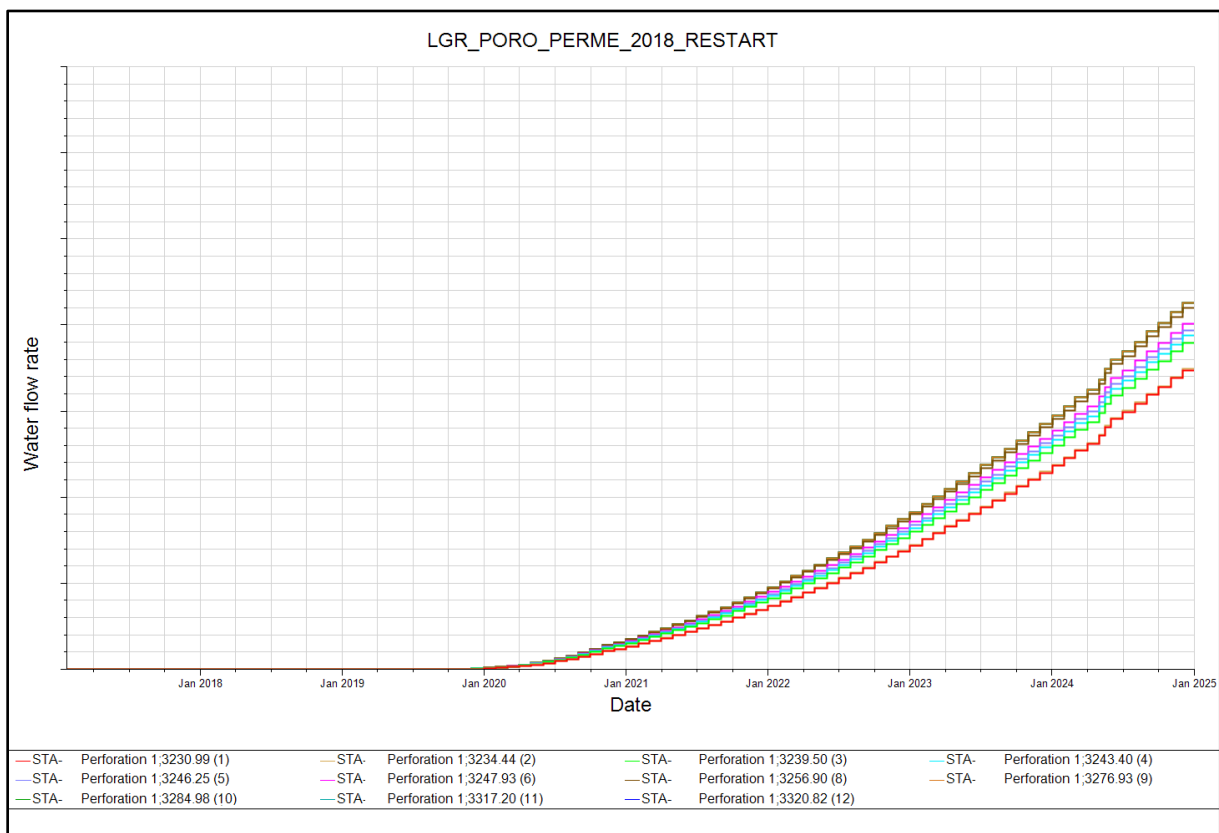


Figure 8-24 Water flow rate from the segments associated with perforation number 1.

Sensitivity Analysis of Reservoir Simulated Production Changes Caused by While-Drilling Updates

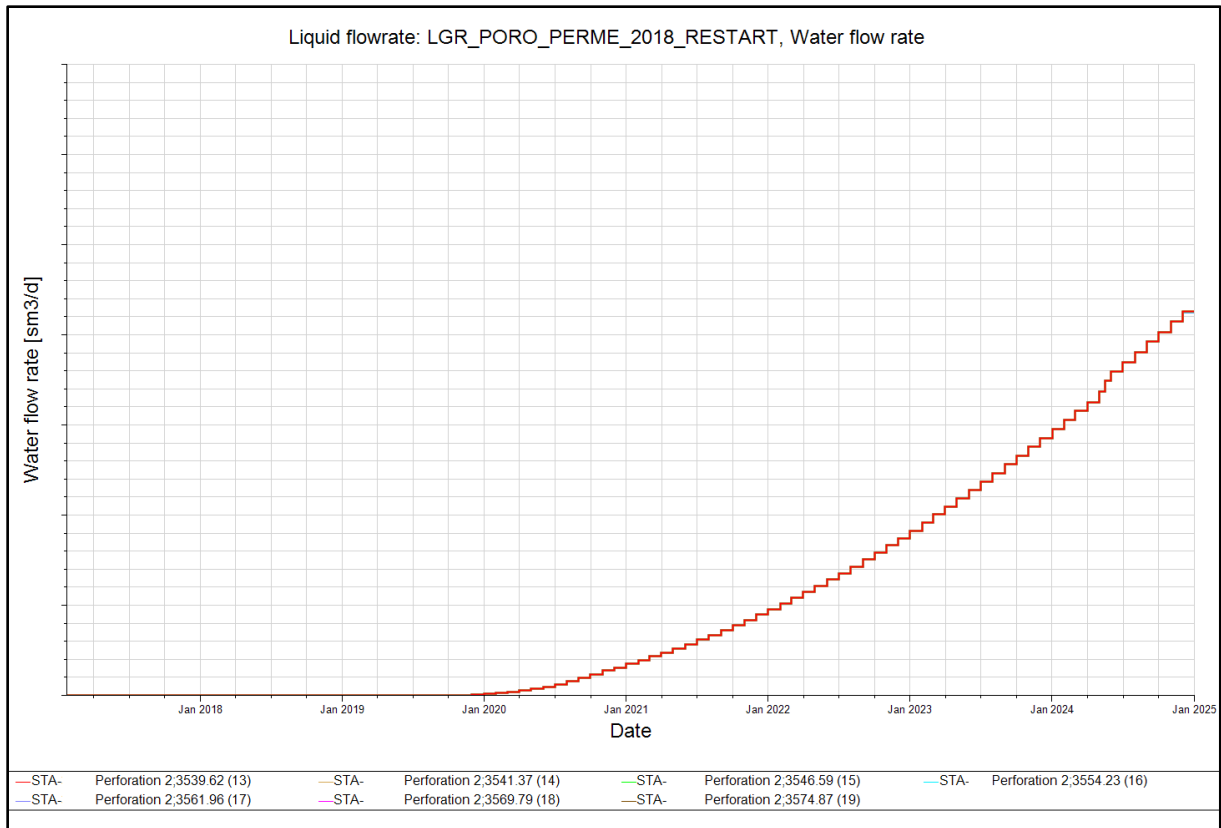


Figure 8-25 Water flow rate from the segments associated with perforation number 2.

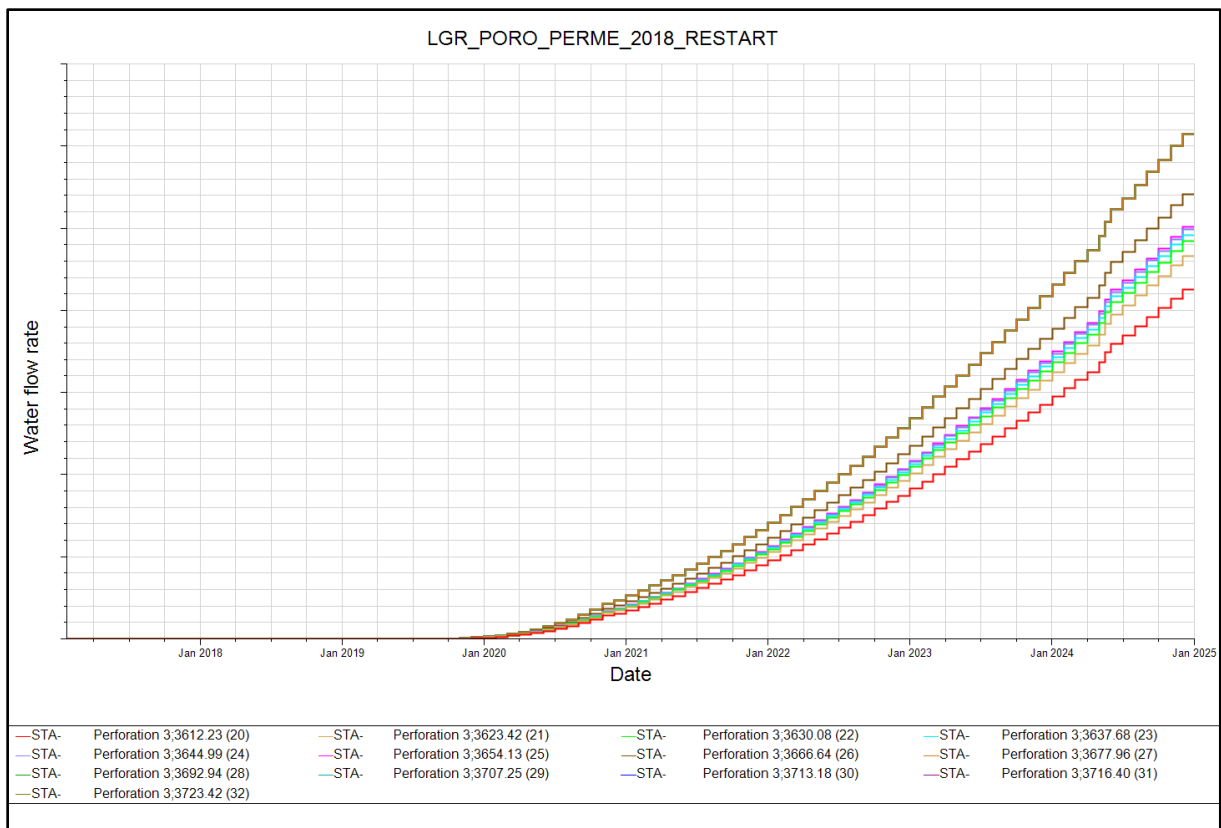


Figure 8-26 Water flow rate from the segments associated with perforation number 3.

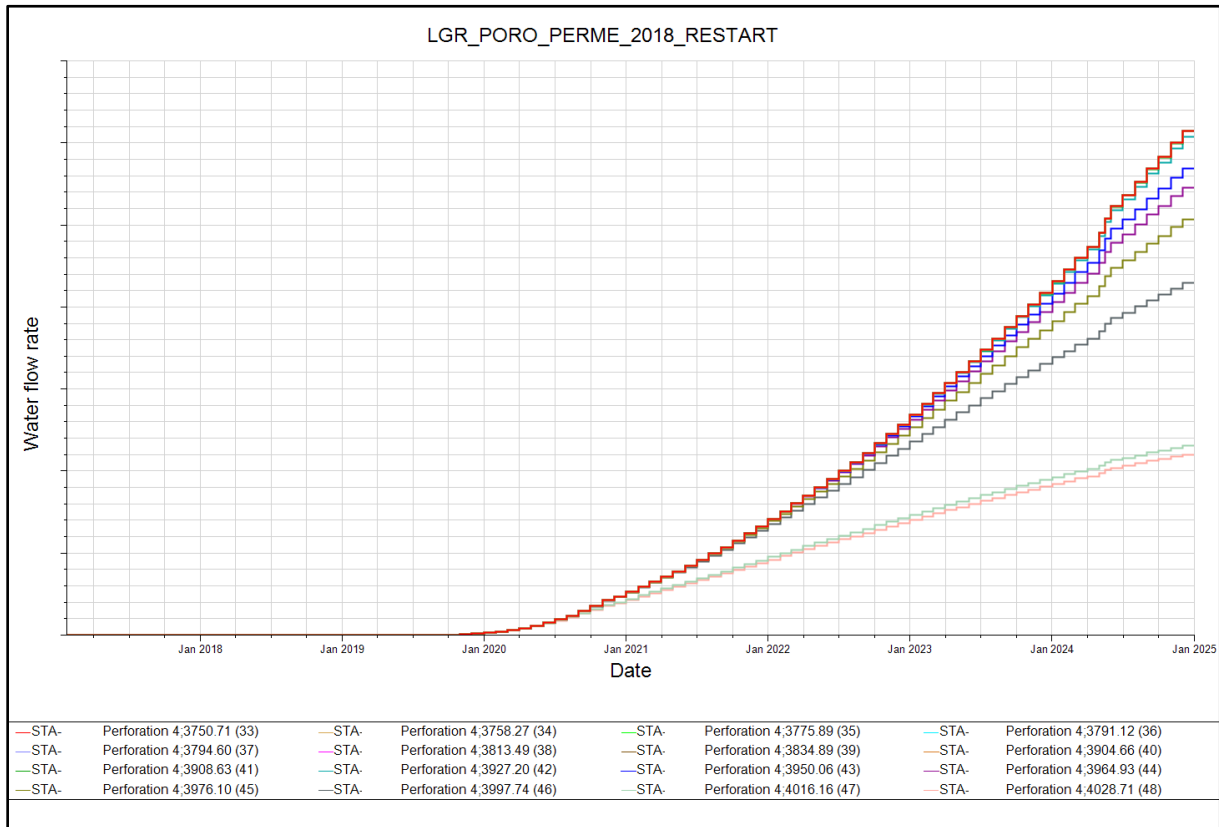


Figure 8-27 Water flow rate from the segments associated with perforation number 4.

Figures below shows the water production located in each one of the perforations. It is shown that the WBT reach all the perforations more or less at the same time. Some segments from perforations number 3 and 4 are the major producer of water. Considering the results, it is possible to confirm that the water front comes laterally from the injector towards the producer.

### 8.5. Updates only within polygon close to the well (Case 4)

Once the update of properties was done in the LGR, a sensitivity study of the extent populated by the new properties was done. Figure 7-7 illustrates the designed polygon with the new porosity and horizontal permeability. The results obtained were the following ones:

### 8.5.1. Pore volume variations

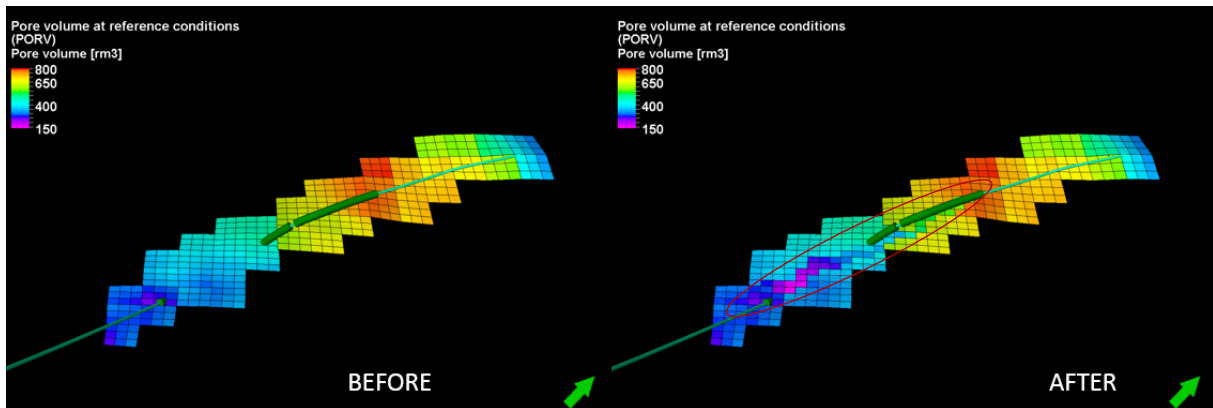


Figure 8-28 Pore volumes before and after the update of the property (layer number 5).

Figure 8-28 illustrates the change in pore volume for layer number 5 in the local grid. A comparison was done before and after the porosity was updated. The mean values for the zone selected changes from  $524 \text{ m}^3$  to  $513 \text{ m}^3$ , which generated a decrease of about 2.1% in this static property. The overall percentage of change in pore volume inside the LGR was 1.4%.

### 8.5.2. Permeability variations

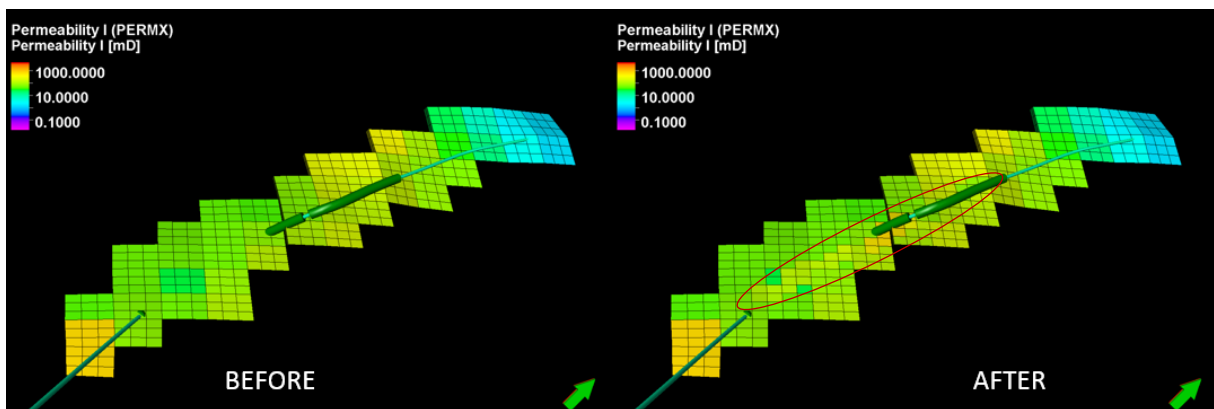


Figure 8-29 Permeability values in  $i$  direction (Layer 5,  $k$  direction).

Comparison between the mean permeability values in layer 5 is shown (Figure 8-29) before and after the update. For the LGR region selected the value changes from  $121.19 \text{ mD}$  to  $143.46 \text{ mD}$ , which is an increase of 15.5%. For  $j$  ( $y$ ) direction, values change in the same way. The overall percentage of change in permeability inside the LGR was 19.7%.

### 8.5.3. Field performance

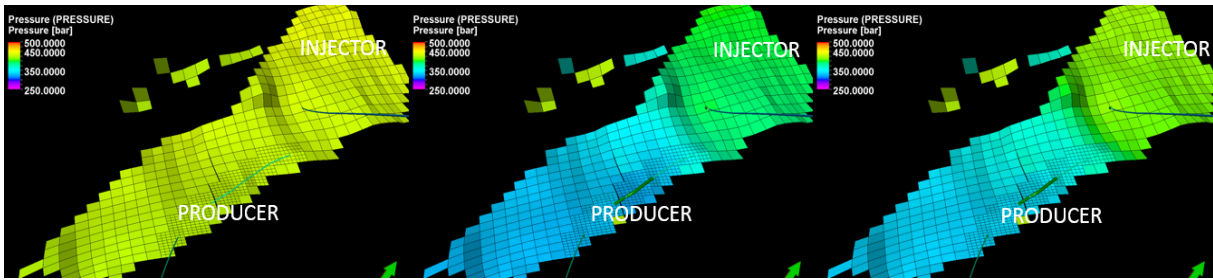


Figure 8-30 Dynamic pressure changes in the years 1999, 2017 and 2025 respectively.

As expected, pressure values are between that of the Base case and that of Case 3 (see Figure 8-2 and Figure 8-20) at the end of the prediction.

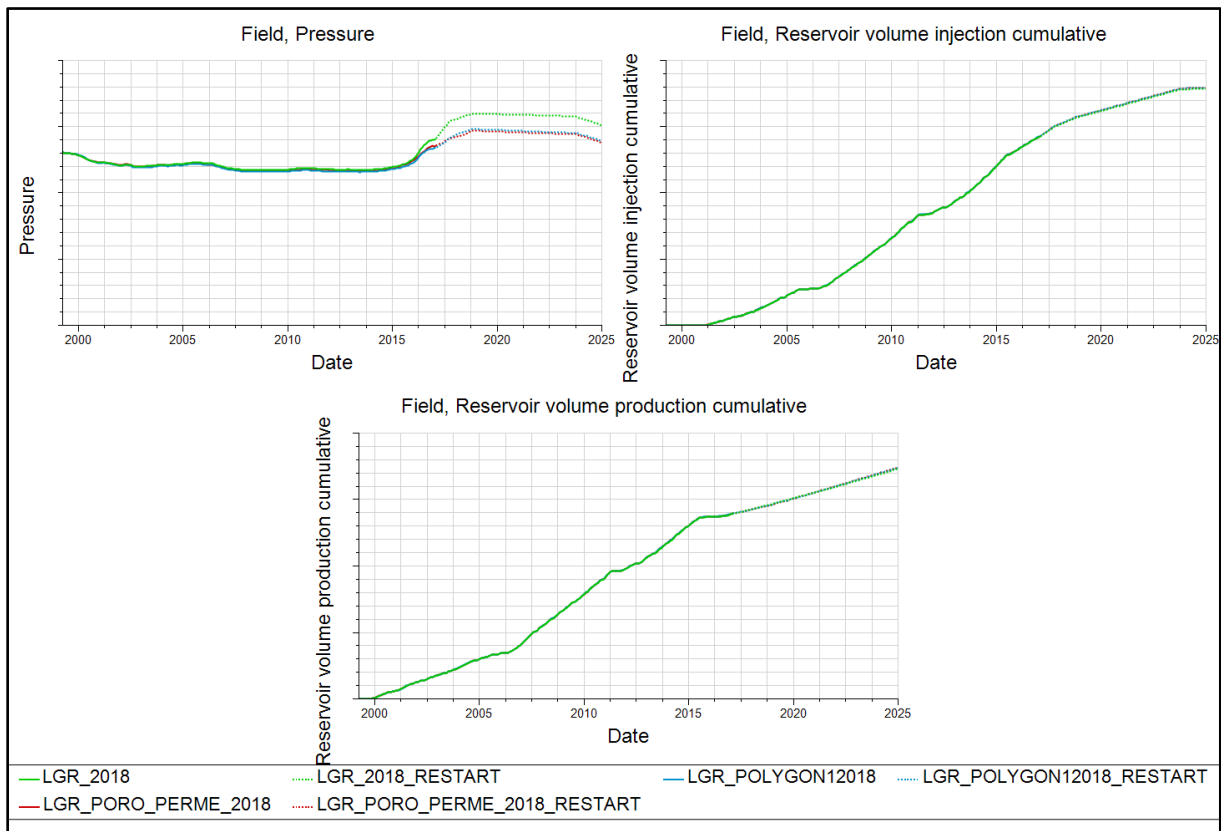


Figure 8-31 Field pressure and, cumulative injection and production for the Base case and Case 4.

Figure 8-31 allows to confirm how important remains the impact of the permeability in the field pressure, also when just a small portion of the LGR is updated with the properties. AS in all the previous scenarios the volume of cumulative injection still being slightly higher than the volume of cumulative production.

### 8.5.4. Bottom hole pressure and production rates in the producer

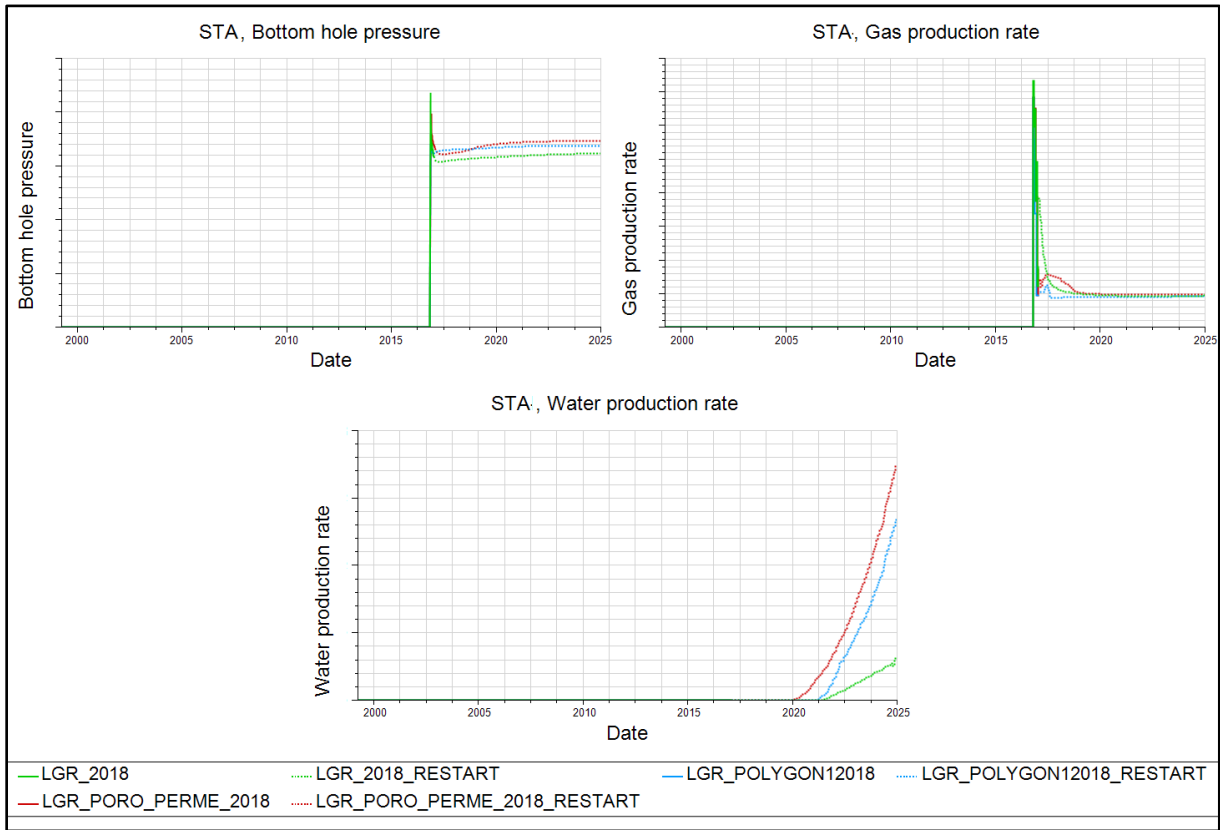


Figure 8-32 Bottom hole pressure and production rates comparison between the Base Case, Case 3 and Case 4.

As expected (Figure 8-32) bottom hole pressure and production rates are concentrated mainly between those of the Base case and those of Case 3. In the case of water production, a water breakthrough is visible around the same date that the Base case.

### 8.5.5. Water front behavior

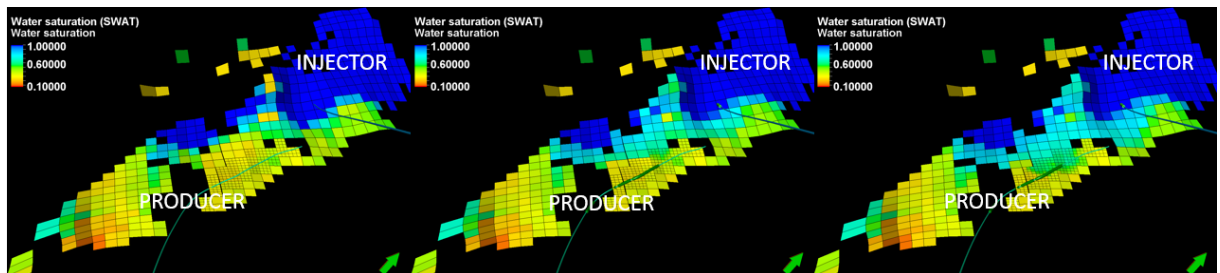


Figure 8-33 Water front behavior in the Case 4 for the years 1999, 2017 and 2025 (layer 8, k direction).

Figure 8-33 shows the water front behavior when both properties are added just in a small sector of the LGR. As in the previous cases, the water moves to the north of the producer

reaching the perforations around the same date that in the Base case but with a high production of water.

### 8.5.6. Water flow rates in each perforation

As described previously, the impact on the water flow rate for each of the perforations was also studied for this case to check in which segments of the perforations the water reached faster during the prediction.

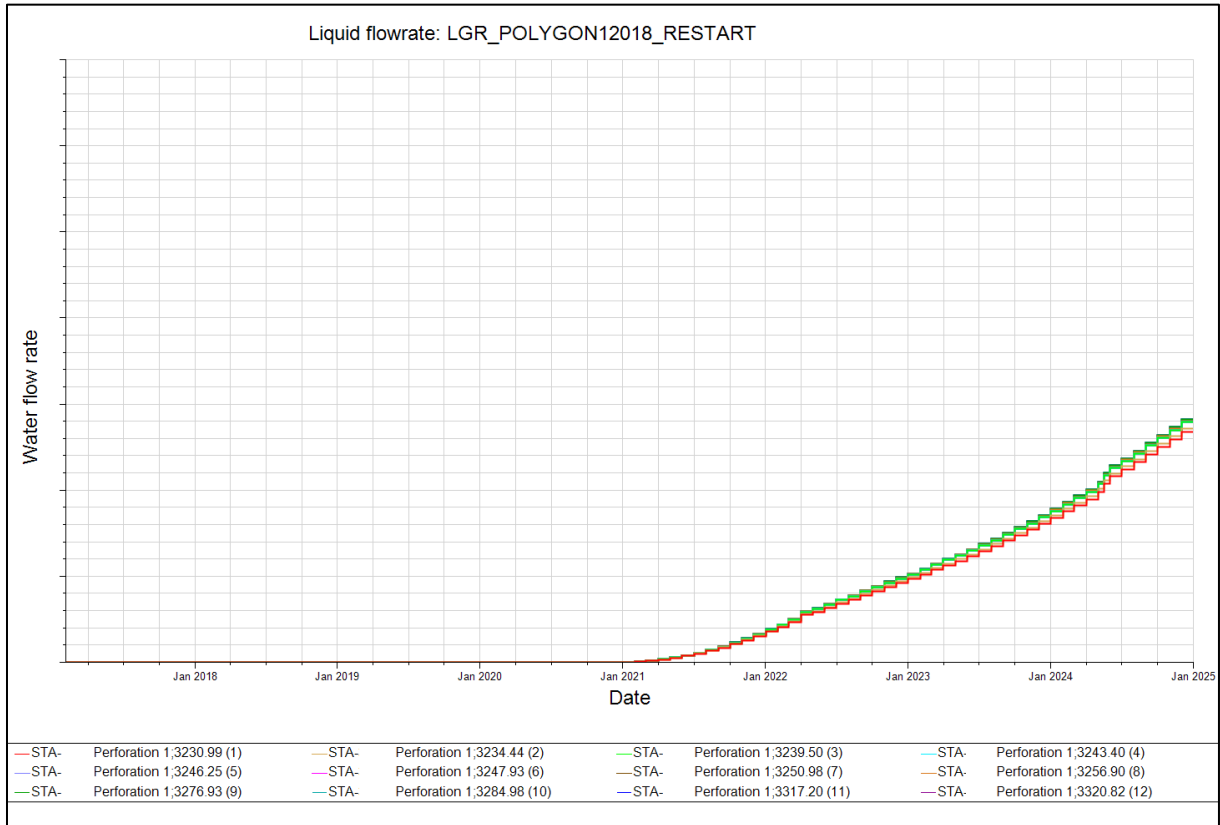


Figure 8-34 Water flow rate for each segment located in the perforation number 1.

Sensitivity Analysis of Reservoir Simulated Production Changes Caused by While-Drilling Updates

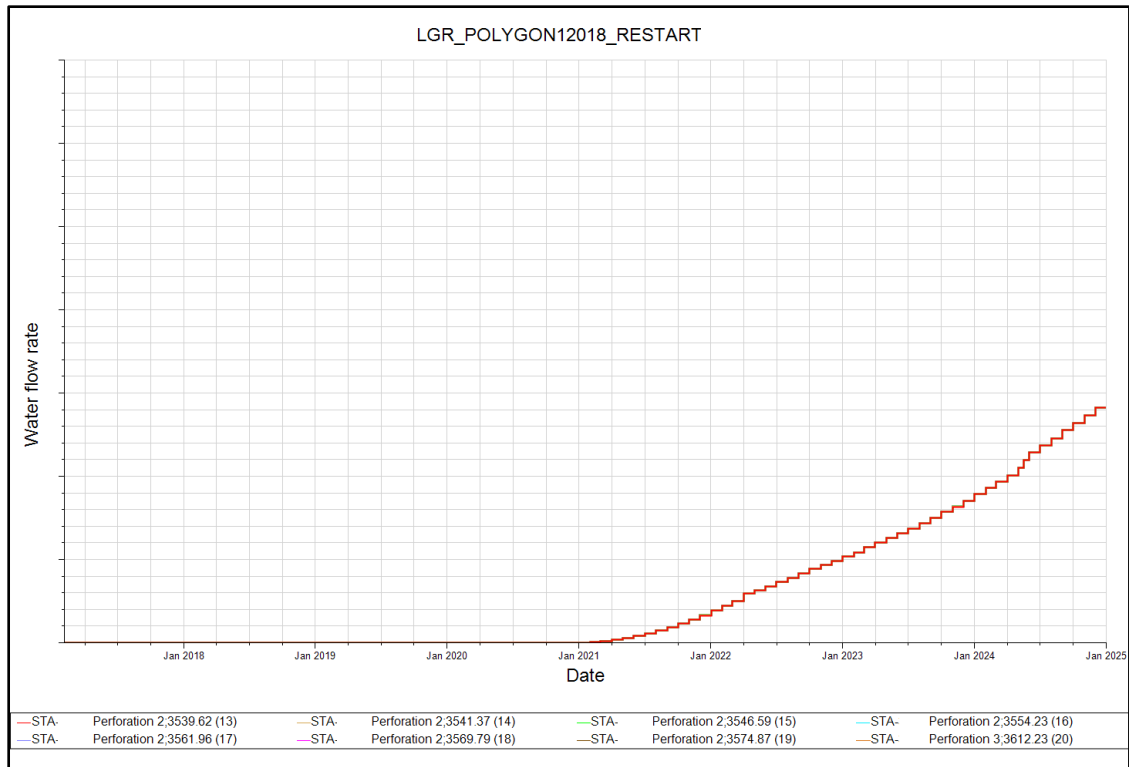


Figure 8-35 Water flow rate for each segment located in the perforation number 2.

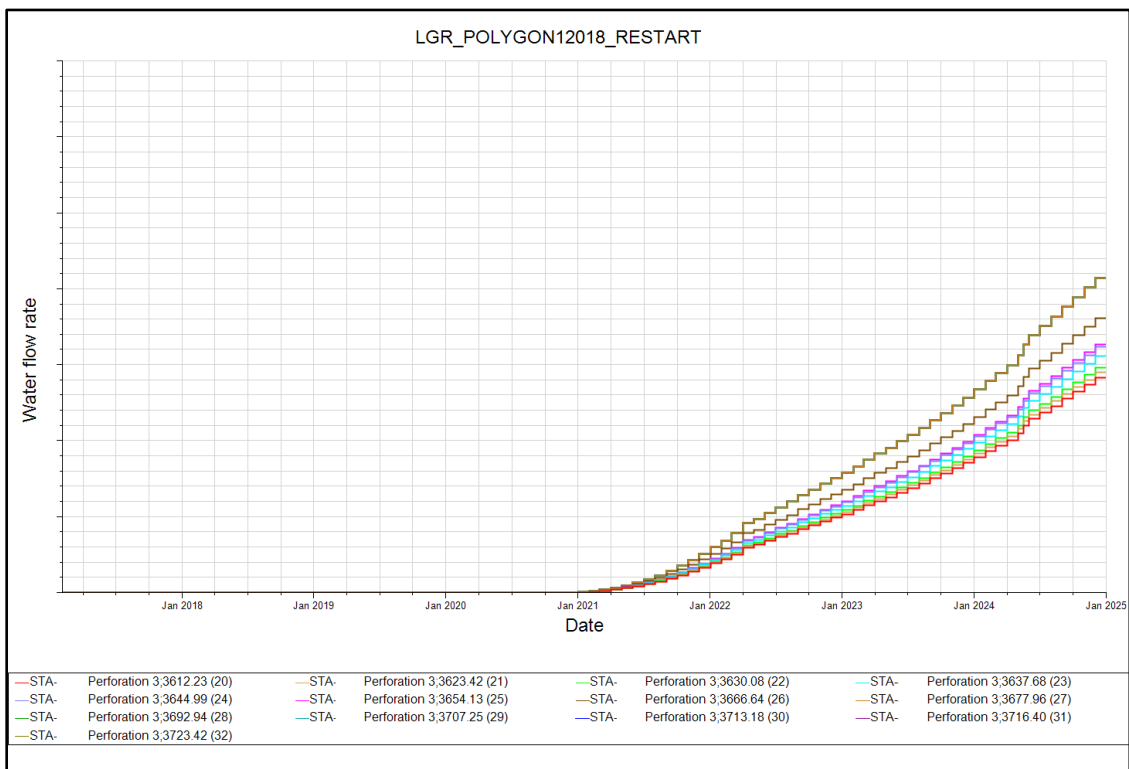


Figure 8-36 Water flow rate for each segment located in the perforation number 3.

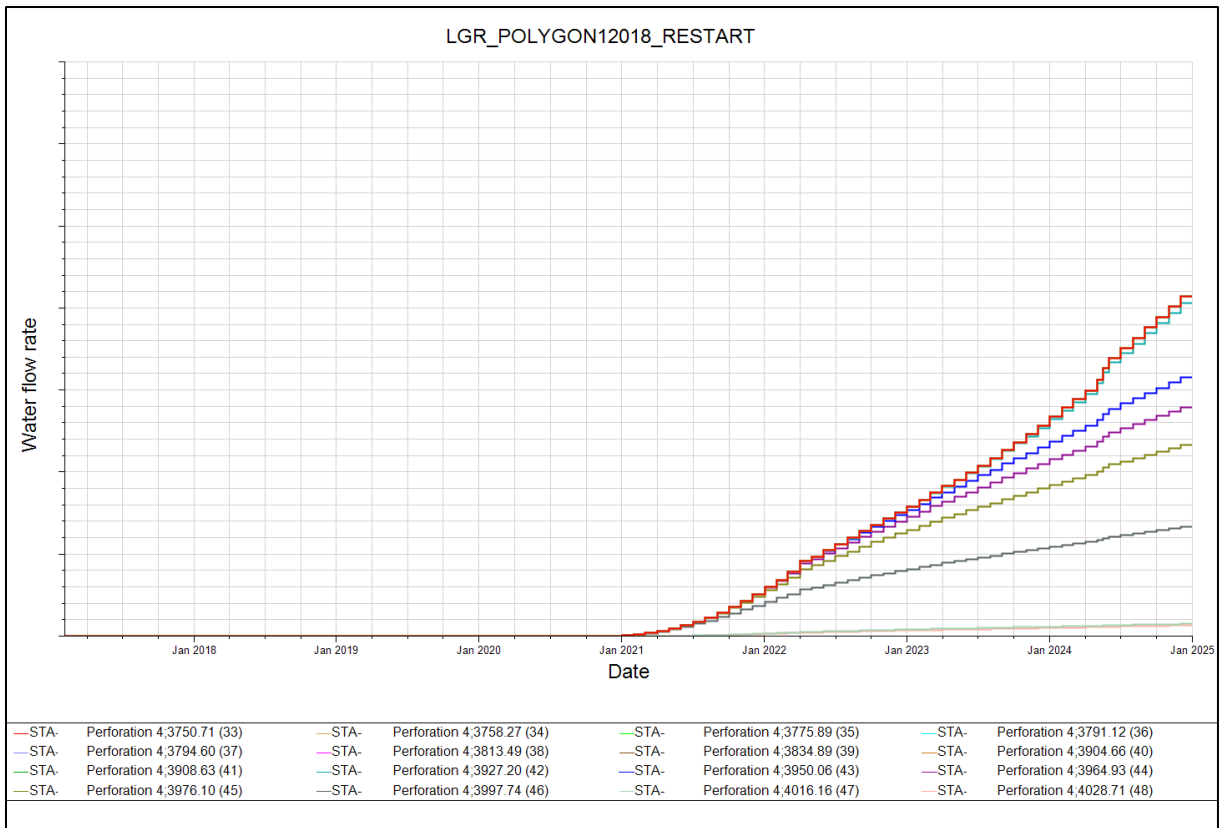


Figure 8-37 Water flow rate for each segment located in the perforation number 4.

Results showed that some segments located in perforations 3 and 4 present a higher production of water when this reaches the producer well. In comparison with the previous scenario, water production behavior is similar but the WBT is later than in the Case 3.

### 8.6. Impacts on the WBT for different perforation scenarios

The following simulation case was considering Case 3, when both properties are modified with the log data in the LGR.

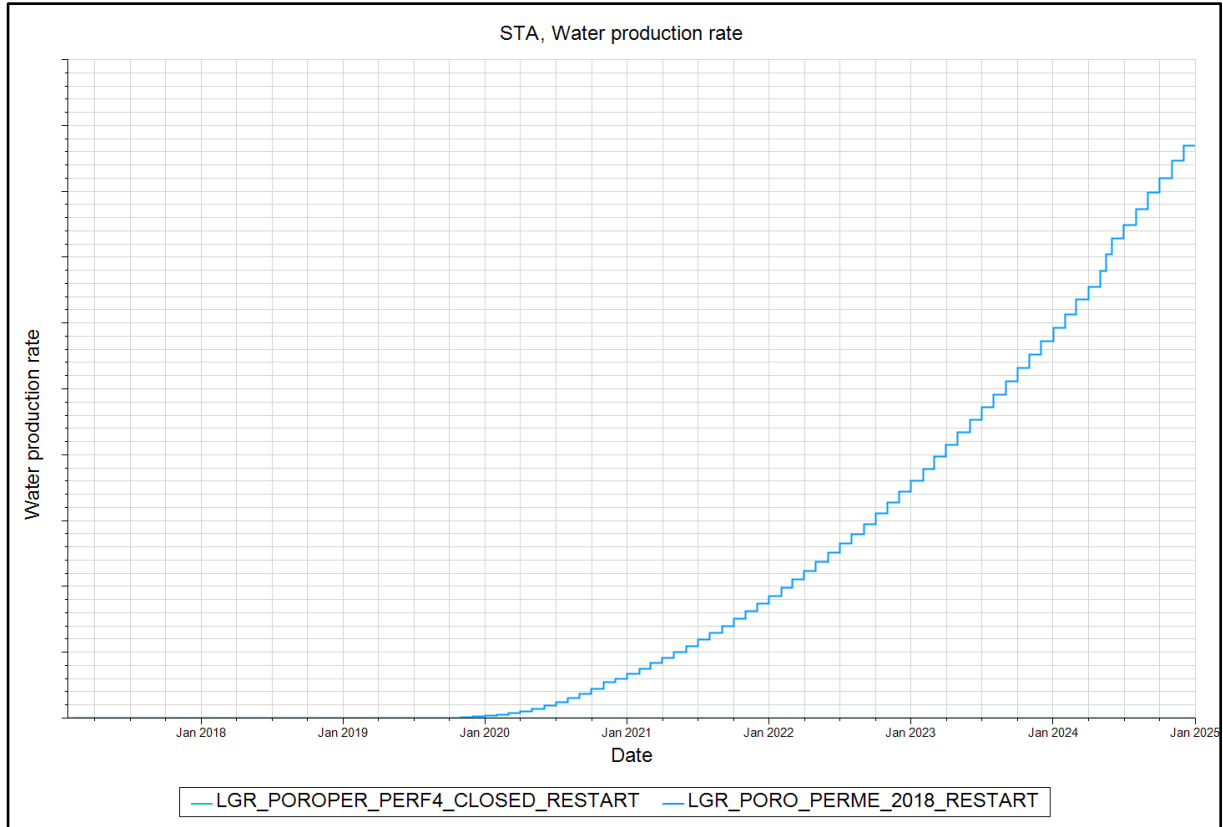


Figure 8-38 Water breakthrough comparison when perforation 4 is closed since the beginning of the production.

Considering perforation 4 to have the segments who showed major production of water when the WBT reaches the well and also because is the perforation that is located nearest to the injector well, this producer zone was closed since the beginning of the production to study the impact. From Figure 8-38 when perforation 4 is closed, it is appreciable a delayed in the WTB. Some traces are shown by the end of 2023 but are not noticeable in the current figure. In order to not close completely this productive interval, other completion options can be taken into consideration.

## 9. DISCUSSION

It is relevant to emphasize that results obtained and illustrated in the previous chapter were obtained using tools developed by Schlumberger Stavanger Research, as is the case of the plugin and workflows created in the Petrel software to understand the dynamic behavior in the reservoir. Multiple case scenarios were presented previously, generating different outcome impacts. The analysis is devoted to the prediction phase. However, because the property modifications were introduced from the beginning of the production, it has to be taken into consideration that the changes also influenced the historic case. That is why there are appreciable differences in both the starting point and the dynamic results in each of the prediction scenarios presented.

The initial run simulations using the previous version of the software showed an anomaly related to the connection transmissibility at the edge of the local grid in the results, mostly for cells located in the north zone of the LGR, possibly due to the complexity of the reservoir. Therefore, it was necessary to move to the version 2018.1 of the INTERSECT simulator to analyze the correct behavior of the dynamic properties for the selected cases.

For the different scenarios when properties were updated, it was checked also the performance of the neighbor producer to determine if this well also contributes to the dynamic changes in the compartment. For each one of the cases, the neighbor producer shows a constant behavior related to the bottom hole pressure, production of gas and there is no appreciable WBT during the prediction time.

It is essential to study the field pressure for the prediction cases. Differences between the Base case (Figure 8-3) and Case 1 (Figure 8-10) are visible. Case 1 shows a slight reduction in field pressure values in comparison with the Base case. An explanation is that porosity is directly proportional to the pore volume, which is aligned with the number of fluids present in the compartment. A reduction in porosity triggers a depletion which can be noticeable as a pressure reduction. Case 2 (Figure 8-15), the effect of the modification of permeability displays a bigger impact on the field pressure. One reason for this effect is associated with the calculation of transmissibility, which can contribute to the flow path behavior in the compartment and thus to a faster depletion. From fluid flow in porous media background (Darcy's Law and Muskat equation (Zhumagulov & Monakhov, 2013)) it is known that permeability is highly connected with dynamic changes in the reservoir, cases in which permeability takes place shows smaller values of  $\Delta P (P_{Re} - P_{wf})$ , this because of the high values of permeability around the well

(Figure 8-17). When both properties are added (Figure 8-21) it is possible to confirm the contribution of the 2 properties in the pressure of the compartment.

In addition, the cumulative injection of fluids is relevant. Due to the fact that in all the cases shown in the results, this value is higher than the cumulative production, values of the dynamic pressure behavior during the prediction time tends to increase. In the Case 3 (Figure 8-20) values are between those of Cases 1 (Figure 8-9) and 2 (Figure 8-15), which is expected when both impacts are combined. Case 4 (Figure 8-30), which is associated to updates only very close to the wellbore, displays a reduction in pressure values in comparison with Case 3 at the end of the prediction due to the smaller extent selected to be modified. A contrast in the dynamic pressure is shown between the north and the south part of the compartment, this is attributed to the presence of a fault crossing from east to west mentioned in the study case (Chapter 6).

Related to production rates, as it was mentioned in the methodology (Chapter 7), the presented forecasts are mainly centered around the high angle production well. For the prediction case, the oil production was used as the main constraint, to evaluate the gas and water behavior during the time of the prediction for the selected cases. For the gas production rate, values of production are shown at the beginning of the prediction in most of the cases (Figure 8-4, Figure 8-11 and Figure 8-32). An explanation of this behavior was displayed in Figure 8-5, where it is clear that the old producer well generated a presence of free gas in the compartment that afterward, is produced by the high angle well when it is open to production.

In comparison with the Base case in which the breakthrough time was around February 2021 (Figure 8-4), Case 1 and Case 2 shows an earlier WBT just a few months ahead. An explanation for this behavior is bearing in mind equation 2.13, used for well testing analysis: Changes over time in water saturation are highly dependent on porosity and permeability updates. This is appreciable when the update of properties is done (Example: Figure 8-12). Considering that the modifications in porosity and permeability are since the time 0 of the production, from equation 2.13, when the study of the effects are done independently, modifications possibly imply that the pressure disturbances travel faster through the porous media and reach the zones of high  $S_w$ , generating an earlier water flow with respect to the Base case. Consequently,  $S_w$  values are higher in the vicinity of the well when the well starts to produce. In addition, it is relevant to mention that the updates were done just around the high angle well, that is why the impacts are not expected to be big in comparison when the total compartment is modified.

In comparison to the individual impacts, Case 3 (Figure 8-22), where both properties are modified at the same time, presents an expected WBT in comparison to the Base case. Based on the theoretical background and the behavior of the properties independently result in water production is consistent. As it was predictable, porosity and permeability updates generated an increase in the water front velocity reaching the well almost a year and a half before that in the Base case. Water flow rates in each one of the perforations show that the water front reaches the producer zones at the same time but with different production rates, perforations 3 and 4 display this, which are the nearest perforations to the injection well.

For Case 4, when just a small area around the well is modified, the WBT comes more or less at the same date of the Base case but with a higher production of water due to the two properties added. Here, the extension of the updated zone plays an important role because it allows to confirm that maybe there is not a significant difference between the WTB but, in terms of pressure and water saturation behavior some effects are shown (Figure 8-30 and Figure 8-33). As expected, values of BHP and gas production rates are between those of the Base case and Case 3. In addition, perforations present a WBT the same date but later than in Case 3, confirming that the flow path behavior is similar to the previous case.

In the current study, the water front behavior moves from the north towards the producer well. However, differences between the cases are focused on the water front velocity approaching the producer well, mainly because of the creation of new flow paths for each of the scenarios. This significant point can be compared in Case 2 (Figure 8-19) with respect to the Base case (Figure 8-7). Because of the heterogeneity in the compartment around the producer well, an increase in the velocity of the water is generated and consequently, the water front accelerates.

In the last part of the results, a study of how fast the water reaches the producer well when perforation 4 is closed was performed. Mainly based on Case 3 (Figure 8-38). Results show that when perforation 4 is closed the WBT is delayed. It is possible to infer that since the perforation 4, which is the closest to the injection well is not producing, new flow paths were generated. A possible completion using control devices would be a strategic option to regulate the water front in some productive zones to maximize the oil production instead of closing the entire perforation.

Although the results of these analyses are very useful to study the future dynamic behavior of the reservoir based on real data obtained by LWD measurements, there is still a degree of

uncertainty associated with the calculation of porosity and permeability in  $x$  and  $y$  from the logs. Empirical equations are used to calculate these final values as it was mentioned in Chapter 5. This can lead to certain inaccuracies. Other relevant points to bring into the discussion are the sector model boundaries and size. Even though reservoir engineers tried carefully to consider all the impacts associated with the communication of the compartment with neighboring areas, it is impossible to model the behavior 100% accurately. On the other hand, it was previously mentioned that kriging methodology was chosen to populate the area selected to modify the properties. This approach was chosen because it was the one that better adjusts with the data available. Considering the restricted number of wells for which data was gathered, that can limit the property modeling in certain zones of the compartment.

After check tuning and convergence effects for the Base case, to consider the proper behavior based on the observed data, it is possible to see a meaningful change in the results based on the ones obtained in the present thesis. Due to the shortage of time, it was not possible to show the results considering the proper tuning in order to be more accurate.

A last important topic to discuss is the extension of the LGR selected for the developed study. This extension was designated in to determine in a more accurate way the path of the fluid flow around the high angle well. In addition to this, to determine which producer zones have major impact related with the time and production of water. Considering the previous arguments may be possible that due to the lack of information, some outlying zones of the local grid refined were not updated with the same quality data that in the nearest part of the well section.

## 10. CONCLUSION AND FURTHER STUDIES

An analysis was done to see how significant updates of static data can be in estimating the future performance of the reservoir. The main part of the analysis was focused on porosity and permeability modifications from real data obtained from wells located in the compartment. All cases considered a local grid refinement (LGR) around the main producer well of this sector.

After the updates of porosity (Case 1), pore volumes tended to be smaller and consequently so was the energy in the sector model. Results showed that this modification generates an early watering out of few months in the producer during the forecasting in comparison with the Base case. In the case of updating the permeability (Case 2), an acceleration in the water front is displayed, but due to the extension of the area updated the early WBT is not very significant in comparison with the Base case. A noticeable increasing on permeability values also contribute to a faster depletion of the compartment.

Update of both properties was done in the static model simultaneously (Case 3). Dynamic results showed an increase in the velocity of the water front, reaching faster the producer well almost a year and a half. This confirms the individual effects of the porosity and permeability when are added in the same scenario. Then a polygon was specified to modify just a small zone of the LGR (Case 4), to determine how the updates in properties influenced the change in static and dynamic properties when the extended area is changed. As expected, values of gas production and BHP were located between those of the Base case and the case with modified properties in the entire local grid (Case 3), keeping the oil production as a constraint. Furthermore, the modification of properties and zones selected to do this has an influence on the displacement and velocity of the water front, this due to the high heterogeneity of the reservoir.

Permeability values in  $i$  and  $j$  direction were calculated from empirical equations. A further study is recommended when values of total permeability can be obtained from the run of a Magnetic Resonance Log (Dunn, Bergman, & LaTorraca, 2002), which allows to do measurements of porosity and thereby, a prediction of permeability values.

In this study, the Base case model considered an LGR around the well. It would be positive if also a sensitivity analysis of the refinement area is done. This with the purpose of not just studying the static updates but also determine how big is the impact when there are several cases with different refinements. Same with the extension selected to populate with new properties. Due to the noticeable contrast between the new properties and the ones from the

original model will be important to study when all the compartment is populated with the new property values in order to have a bigger impact on the results.

Moreover, during the study, a determination of the effect on the water production for each one of the producer zones and the effect when one of this one is closed was done. This considering that the water front was moving from the injector to the north of the producer. From the results obtained, a project dedicated to a further study related with possible advanced well completion technologies to control and manage in a more optimal way the water influx towards the high angle producer well is suggested. These technologies include intelligent well completions, autonomous inflow control devices or ICD (Inflow control devices). Currently, SSR (Schlumberger Stavanger Research) is working on a study devoted to ICD optimization for current and future producer wells in this reservoir considering newly available deed reading resistivity data obtained with the so-called GeoSphere tool. These studies can generate a positive impact not just with topics related to water encroachment and reductions of bypassed reserves, but future cost saving associated with problems with rig interventions (Armstrong & Jackson, 2001) (Ellis et al., 2009).

Some uncertainties are associated related to the impact on the modification of the tuning and convergence in the results. Presently, the research group is working in select the correct tuning considering the observed data in order to have results with a higher degree of certainty. Additionally, a further study doing some sensitivity analysis to the prediction strategy selected in the current thesis will be interesting to see how this change the dynamic properties and the production rates.

A final aspect to be addressed is related with the structural updates. The present thesis did not cover this part due to the time demanding to gather all the necessary information to visualize the impacts in a new sector model, applying petrophysical modeling along all the compartment. The next sub-section explains the progress related to this further work:

### **10.1. DepoGrid Construction**

With the purpose to build and characterize accurately the considered compartment, focusing on the structural and stratigraphy information, the latest version of Petrel E&P software (2018) supports a new type of grid called DepoGrid. This grid type is very useful for modeling complex structures. As a result, the dynamic performance of the compartment can be assessed in more detail.

To build a DepoGrid, seismic interpretation is done first to create the surfaces and perform the fault framework modeling. Data obtained with the GeoSphere mapping-while-drilling tool, then allow to determinate subsurface bedding and fluid contacts close to wells to update the reservoir static data and the selection of main faults. Following this, the 3D structural framework is developed and the Depospace that consist of the flattened representation of the structural modeling is done, finally, the DepoGrid is created. This further study tries to cover not just the property updating but also the structural part, which can honor the real structure in the subsurface in the presence of tilted fault blocks and intersecting faults. Future comparisons can be done with the current study to conclude how big the impact of both structural and property updates is. Currently, the project is in the stage of finding the best way to do the property population.

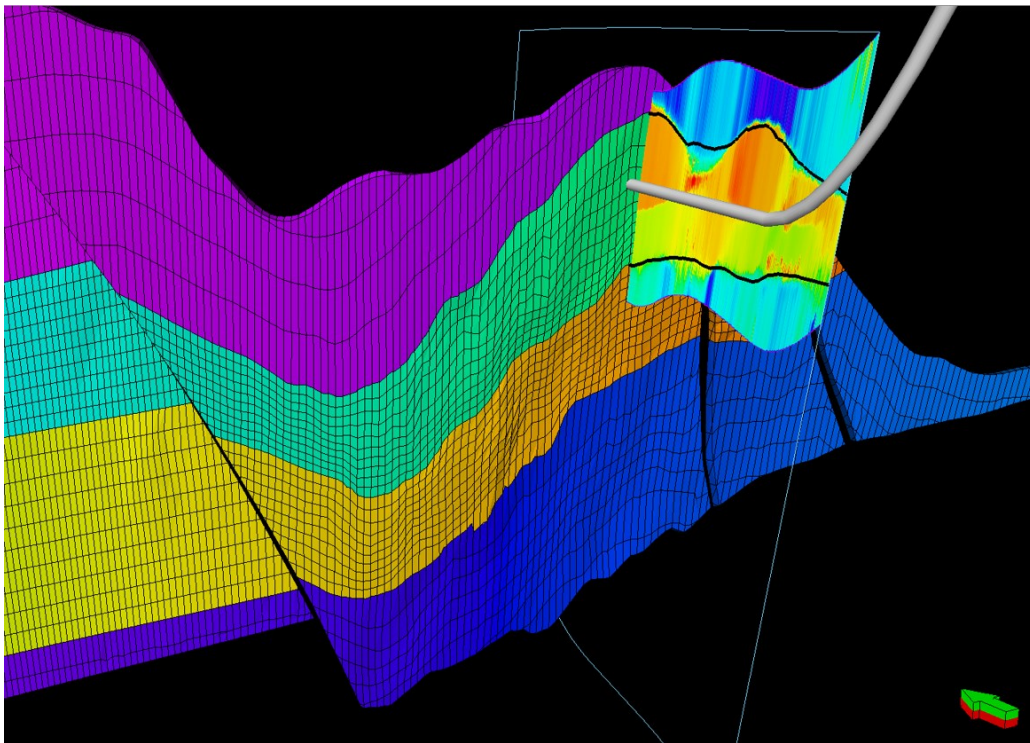


*Figure 10-1 Construction of the DepoGrid for the sector model (Marie Etchebes, 2018)*

## 11. REFERENCES

- Archie, G. E. (1942). The electrical resistivity log as an aid in determining some reservoir characteristics. *Transactions of the AIME*, 146(01), 54-62.
- Armstrong, A. C., & Jackson, M. D. (2001). *Management of water breakthrough using Intelligent Well Technology*. Paper presented at the Offshore Technology Conference.
- Bonner, S., Burgess, T., Clark, B., Decker, D., Orban, J., Prevedel, B., . . . White, J. (1993). Measurements at the bit: a new generation of MWD tools. *Oilfield Review*, 5, 44-54.
- Cordazzo, J., Maliska, C. R., & Silva, A. (2002). *Interblock transmissibility calculation analysis for petroleum reservoir simulation*. Paper presented at the Proceedings from the 2nd Meeting on Reservoir Simulation.
- Da Veiga, S., & Ravalec-Dupin, L. (2010). *Rebuilding existing geological models*. Paper presented at the SPE EUROPEC/EAGE Annual Conference and Exhibition.
- David Allen, D. B., David Best, Brian Clark, Ian Falconer, Jean-Michel Hache, Craig Klenitz, Marc Lesage, John Rasmus, Claude Roulet and Peter Wraight (1989). Logging While Drilling. *Oilfield Review Schlumberger*, 14.
- Dunn, K.-J., Bergman, D. J., & LaTorraca, G. A. (2002). *Nuclear magnetic resonance: Petrophysical and logging applications* (Vol. 32): Elsevier.
- Ellis, T., Erkal, A., Goh, G., Jokela, T., Kvernstuen, S., Leung, E., . . . Vorkinn, P. B. (2009). Inflow Control Devices—Raising Profiles. *Oilfield Review*, 21(4), 30-37.
- Ertekin, T., Abou-Kassen, J. H., & King, G. R. (2001). *Basic applied reservoir simulations*: Society of Petroleum Engineers.
- Etchebes Marie, S. S. R. (2018). DepoGrid Construction, Sector Model.
- Fanchi, J. R. (2002). *Shared earth modeling*: Gulf Professional Publishing.
- Fanchi, J. R. (2005). *Principles of applied reservoir simulation*: Elsevier.
- Gilman, J. R., & Ozgen, C. (2013). *Reservoir simulation: history matching and forecasting*: Society of Petroleum Engineers Richardson, TX.
- Griffiths, R. (2009). *Well placement fundamentals*: Schlumberger.

- Griffiths, R. (2010). *EcoScope User's Guide*: Schlumberger.
- Islam, M. R., Mousavizadegan, S. H., Mustafiz, S., & Abou-Kassem, J. H. (2010). *Advanced Petroleum Reservoir Simulation*. Hoboken, UNITED STATES: Wiley.
- Kamal, M. M., & Abbaszadeh, M. (2009). Transient well testing. *SPE Monogr*, 23.
- Landa, J. L., & Güyagüler, B. (2003). *A methodology for history matching and the assessment of uncertainties associated with flow prediction*. Paper presented at the SPE Annual Technical Conference and Exhibition.
- Lie, K.-A. (2014). An introduction to reservoir simulation using MATLAB: user guide for the Matlab Reservoir Simulation Toolbox (MRST). SINTEF ICT. In: Department of Applied Mathematics Oslo, Norway.
- Lie, K.-A., & Mallison, B. T. (2013). Mathematical models for oil reservoir simulation. *Encyclopedia of Applied and Computational Mathematics*, 1-8.
- Manchuk, J., Neufeld, C., & Deutsch, C. V. (2007). Petrel Plugins for Declustering and Debiasing. *Centre for Computational Geostatistics*, 9, 403.
- Mattax, C. C., & Dalton, R. L. (1990). Reservoir Simulation (includes associated papers 21606 and 21620). *Journal of Petroleum Technology*, 42(06), 692-695.
- Pedersen, S., Tennebo, P., Sonneland, L., & Carrillat, A. (2005). Real time update of a reservoir property model in geosteering applications. In *SEG Technical Program Expanded Abstracts 2005* (pp. 1374-1377): Society of Exploration Geophysicists.
- Saleri, N. G. (1993). Reservoir performance forecasting: acceleration by parallel planning. *Journal of Petroleum Technology*, 45(07), 652-657.
- Schlumberger. (2017a). INTERSECT High-Resolution Reservoir Simulator.
- Schlumberger. (2017b). Petrel E&P Software Platform. In.
- Shtun, S. Y., Golenkin, M. Y., Shtun, A., Shabalinskaya, D., Cheprasov, A., Kuzakov, V., . . . Zolotoi, N. (2017). *New Approach to Offshore Field Development in Russia: Ultra Deep LWD Measurements for Accurate 3D Reservoir Model Update*. Paper presented at the SPE Russian Petroleum Technology Conference.
- Struijk, A., & Green, R. (1991). The Brent Field, Block 211/29, UK North Sea. *Geological Society, London, Memoirs*, 14(1), 63-72.

Tiab, D., & Donaldson, E. C. (2015). *Petrophysics: theory and practice of measuring reservoir rock and fluid transport properties*: Gulf professional publishing.

Wasserman, M. (1987). *Local grid refinement for three-dimensional simulators*. Paper presented at the SPE Symposium on Reservoir Simulation.

Ye, S.-J., & Rabiller, P. (2000). *A new tool for electro-facies analysis: multi-resolution graph-based clustering*. Paper presented at the SPWLA 41st annual logging symposium.

Zhumagulov, B., & Monakhov, V. (2013). *Fluid dynamics of oil production*: Elsevier.

## Appendix I

This appendix displays two relevant windows related with the completion and segmentation of the high angle well. Figure 11-1 displays the Completion manager considering the casing selected and the perforations in the well with the respective creation dates. Base on this information the simulator includes the selected well events at the specific time designated.

Well name	UWI	Category	Type	Name	Start date	Top from	Top offset	Bottom from
Side Track		Borehole	Borehole	Borehole	08/31/2016 00:00:00	Start of well traj	0.00	End of well
Side Track		Casing	Casing string	Casing 1	08/31/2016 00:00:00	Start of well traj	0.00	Well c
Side Track		Casing	Liner string	Liner 1	09/03/2016 00:00:00	Well datum	3098.76	Well c
Side Track		Casing	Liner part	Liner 1:1	09/03/2016 00:00:00	Well datum	3098.76	Well c
Side Track		Workovers	Perforation	Perforation 1	09/04/2016 00:00:00	Well datum	3231.09	Well c
Side Track		Workovers	Perforation	Perforation 2	09/04/2016 00:00:00	Well datum	3539.19	Well c
Side Track		Workovers	Perforation	Perforation 3	09/04/2016 00:00:00	Well datum	3604.89	Well c
Side Track		Workovers	Perforation	Perforation 4	09/04/2016 00:00:00	Well datum	3747.61	Well c
Side Track		Workovers	Perforation	Perforation 5	09/04/2016 00:00:00	Well datum	3963.21	Well c

Name	Value
<b>Depth</b>	
Bottom from	Well datum
Bottom MD	4572.23
Bottom offset	4572.23
Bottom SSTVD	2899.83
Top from	Well datum
Top MD	3098.76
Top offset	3098.76
Top SSTVD	2777.55
<b>Diameters</b>	
Coupling outer diameter	7.65600
Drift diameter	6.33100
Inner diameter	6.45600
Outer diameter	7.00000
<b>General</b>	
Category	Casing
Completion length	1473.47
End date	
Equipment ID	C-API-7.000/1-55/20.0
Name	Liner 1:1
Start date	09/03/2016 00:00:00
Type	Liner part
UWI	
Well folder	Wells
Well name	Side Track

Figure 11-1 Completion of the high angle well (producer well).

Figure 11-2 shows the selected pressure drop components for the wells involved in the simulation cases. As it can be seen, friction and acceleration are the key factor for this calculation. It is important to remember that some wells are not located in the compartment but are still linked with the dynamics in this region.

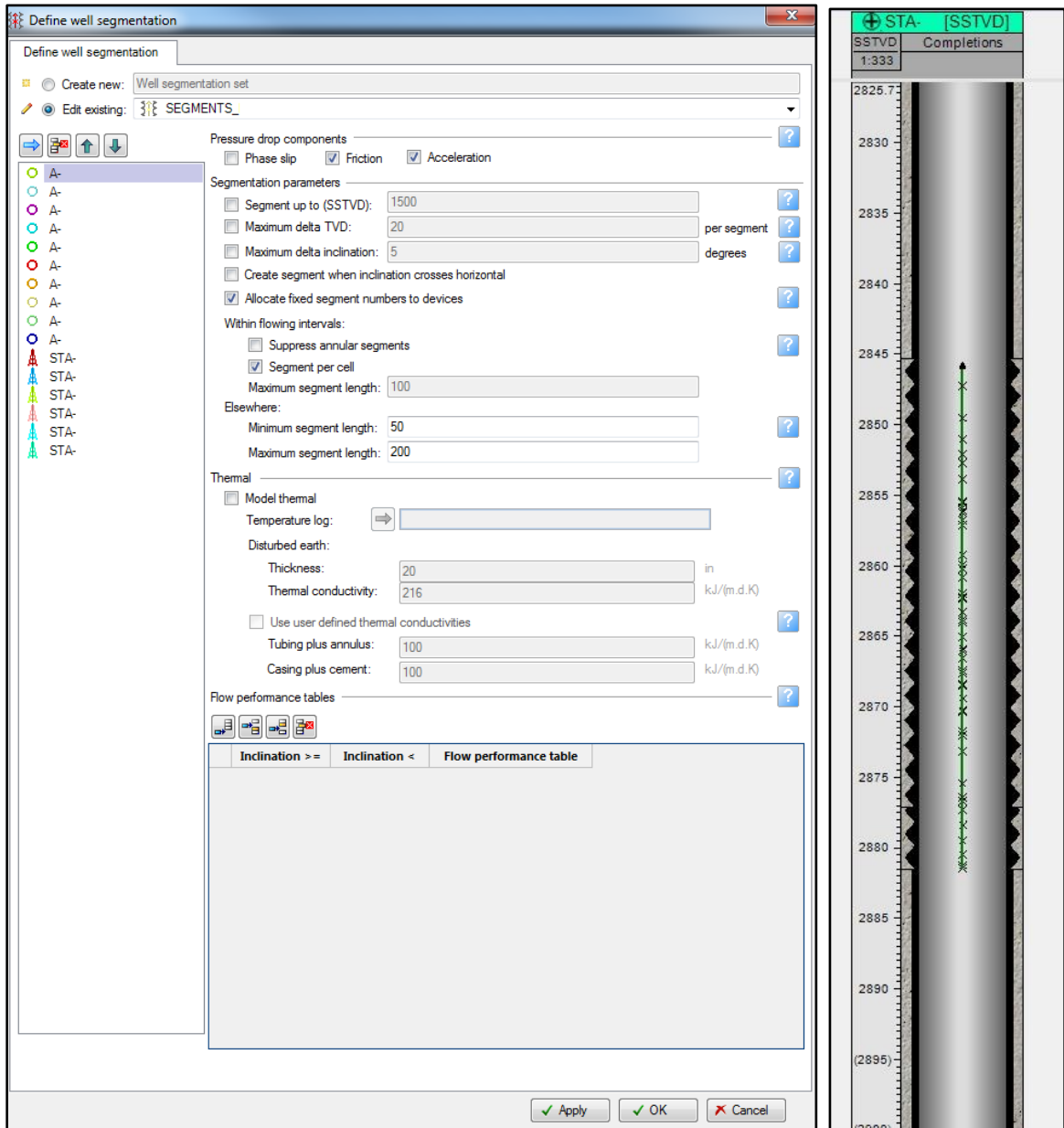


Figure 11-2 Well segmentation setup for the simulation runs.

## Appendix II

```
#####
# IXFVERSION: 2017.1 Petrel
#####
```

### MODEL\_DEFINITION

```
PropertyIdService {
  UnitSystem=ECLIPSE_METRIC
}
```

```
DATE "20-Jan-2017"
#TIME 6504.0
```

```
FluidSourceExternal "SA_INJ" {
  Phase=GAS
  AvailableRate=DoubleProperty(0 GAS_FLOW_RATE)
}
```

```
Group "1" {
  Members=[Well("") Well("INJECTOR") Well("PRODUCER") Well("")]
  InjectionStream=Well("")
}
```

```
Group "2" {
  Members=[Well("") Well("") Well("") Well("") Well("") Well("") Well("") Well("")]
}
```

```
Group "3" {
  Members=[Group("2")]
}
```

```
Group "4" {
  Members=[Group("1") Group("3")]
}
```

```
Group "SA_PROD" {
}
```

```
Group "SA_INJ" {
  InjectionStream=FluidSourceExternal("SA_INJ")
  OverrideWellInjectionStream="True"
}
```

```
Group "5" {
  Members=[Group("4") Group("SA_PROD") Group("SA_INJ")]
}
```

```
GuideRateBalanceAction "GroupControl" {
```

```

Constraints=["GAS_INJECTION_RATE(Group('5')) == 8000000"
"GAS_PRODUCTION_RATE(Group('5')) == 18300000"
"GAS_PRODUCTION_RATE(Group('4')) == 15000000"
"GAS_PRODUCTION_RATE(Group('3')) == 8000000"]
  DefaultGuideRateType=POTENTIAL
}

Strategy "GroupControlStrategy" {
  BalancingAction=GuideRateBalanceAction("GroupControl")
}

Group "GEXP" {
  Members=[Group("5")]
}

Group "Field" {
  Members=[Group("GEXP")]
}

}

Well "INJECTOR" {
  Type=WATER_INJECTOR
  Constraints=[
    data          property
    1500 WATER_INJECTION_RATE
    600 INJECTION_BOTTOM_HOLE_PRESSURE
    100 PRODUCTION_BOTTOM_HOLE_PRESSURE
  ]
  InjectionStream=UNSET
  HistoricalControlModes=UNSET
  HistoricalData=UNSET
}

Well "PRODUCER" {
  Constraints=[
    data          property
    150 OIL_PRODUCTION_RATE
    500 WATER_PRODUCTION_RATE
    1500000 GAS_PRODUCTION_RATE
    100 PRODUCTION_TUBING_HEAD_PRESSURE
    600 INJECTION_BOTTOM_HOLE_PRESSURE
    100 PRODUCTION_BOTTOM_HOLE_PRESSURE
  ]
  HistoricalControlModes=UNSET
  HistoricalData=UNSET
  TubingHydraulicsTableDevice {
    PressureTable="A16-VLPN 45"
  }
}

```

**Appendix III**

```
#####
# IXFVERSION: 2017.1 Petrel
#####
```

**MODEL\_DEFINITION**

```
RockMgr {
  HorizontalEndPointScaling="True"
  VerticalEndPointScaling="True"
}
```

**TwoPhaseSaturationFunction "Saturation function" {**

OilWaterFunction [			
WaterSaturation	WaterRelPerm	OilRelPerm	CapPressure
0.1	0	1	63
0.119	3e-05	0.967395	50
0.138	0.000176	0.922387	41
0.156	0.000499	0.870268	35
0.175	0.001052	0.813124	30
0.194	0.001888	0.752598	26
0.213	0.00306	0.690182	23
0.231	0.004623	0.627256	20
0.25	0.006634	0.565068	18
0.269	0.009154	0.504705	16
0.288	0.012245	0.447064	14
0.306	0.015973	0.392838	13
0.325	0.020408	0.342516	11
0.344	0.02562	0.296393	10
0.363	0.031682	0.254599	9.4
0.381	0.038671	0.21712	8.6
0.4	0.046662	0.183831	7.8
0.419	0.05573	0.154525	7.2
0.438	0.065951	0.128938	6.6
0.456	0.077396	0.106774	6
0.475	0.090133	0.087719	5.6
0.494	0.104222	0.071459	5.1
0.513	0.119718	0.057686	4.7
0.531	0.136662	0.046107	4.4
0.55	0.155084	0.036451	4
0.569	0.174997	0.028466	3.7
0.588	0.196398	0.021924	3.4
0.606	0.219265	0.016619	3.2
0.625	0.243551	0.012368	2.9
0.644	0.269191	0.009007	2.7
0.663	0.296092	0.006391	2.5
0.681	0.324139	0.004395	2.3
0.7	0.353196	0.002906	2.2
0.719	0.383105	0.001829	2
0.738	0.413686	0.001078	1.8

Sensitivity Analysis of Reservoir Simulated Production Changes Caused by While-Drilling Updates

0.756	0.444749	0.000581	1.7
0.775	0.476089	0.000275	1.6
0.794	0.507494	0.000106	1.4
0.813	0.538754	2.8e-05	1.3
0.831	0.569656	3e-06	1.2
0.85	0.6	0	1.1
0.99	1	0	0.49
1	1	0	0

} ]